A narrative review: narrow-band imaging endoscopic classifications

Qingya Yang[1#], Zhimei Liu[2#], Hui Sun[1], Fangdong Jiao[1], Bing Zhang[1], Jun Chen[3]

[1]Department of Urology, Qilu Hospital (Qingdao), Cheeloo College of Medicine, Shandong University, Qingdao, China; [2]Department of Clinical Medicine, Qingdao Medical College, Qingdao University, Qingdao, China; [3]Department of Urology, Qilu Hospital, Cheeloo College of Medicine, Shandong University, Jinan, China

Contributions: (I) Conception and design: Q Yang, J Chen; (II) Administrative support: F Jiao, B Zhang; (III) Provision of study materials or patients: Z Liu, H Sun; (IV) Collection and assembly of data: Z Liu, Q Yang; (V) Data analysis and interpretation: Q Yang, Z Liu; (VI) Manuscript writing: All authors; (VII) Final approval of manuscript: All authors.

[#]These authors contributed equally to this work.

Correspondence to: Jun Chen. Department of Urology, Qilu Hospital, Cheeloo College of Medicine, Shandong University, 107 Wenhua West Street, Jinan 250000, China. Email: chenjunxinxiang@163.com.

Background and Objective: With the development of endoscopic techniques, narrow-band imaging (NBI) has been widely used in the diagnosis of various types of diseases. NBI can detect mucosal lesions at an early stage and different classification strategies have been established to help clinicians in disease diagnosis. However, there is currently no consensus for the classification criteria. This report summarizes the current classifications of diseases using NBI, so as to provide a comprehensive understanding of the various manifestations of mucosal lesions under NBI, and to promote the development of more practical NBI classifications.

Methods: The PubMed database was searched for English language articles published between January 1994 and November 2021 using the keywords 'narrow band imaging', 'NBI', and 'classification'.

Key Content and Findings: We systematically summarized the NBI classifications and manifestations of different diseases. The morphology of the mucosa and vessels was used as the basis of most classifications. These classifications are mainly helpful to distinguish benign and malignant tumors and to detect early neoplastic lesions.

Conclusions: This review summarized existing NBI classifications for different systems. These classifications will be updated as the understanding of diseases increases and new optical techniques become available to better assist doctors in making clinical decisions.

Keywords: Narrow-band imaging (NBI); classifications; cancer; endoscopy; diagnosis

Introduction

Cancer is a major cause of death worldwide and remains a major public health threat (1-3), with a predicted 34 million annual global cases by 2070 (1). It has been widely accepted that the early detection and effective treatment of cancer can decrease the mortality rate (4-6). Therefore, different guidelines have been established to efficiently and effectively detect cancer (7).

A variety of diagnostic methods have been used in clinical practice, including advanced endoscopic

imaging technology, which is a minimally invasive and intuitive diagnostic method used for early detection and identification of various types of cancer (8-11). Narrow band imaging (NBI) is a powerful tool for the diagnosis of disease as it enables clear visualization of the surface of the capillary vessels. Indeed, numerous studies have shown that NBI can improve the precision of tumor diagnosis (12-17).

With increasing research, multiple NBI endoscopic classifications have been established based on different organs. These classifications show differences as well as similarities between organs. Comparing different classifications can provide a reference for diseases that have no NBI classification, such as bladder tumors; it can also provide clues for further improving the existing classifications. Since all classifications are based on the same NBI technique, it may be possible to identify a general classification feature. However, until now, there has been no comprehensive review on this topic. Herein, we present a detailed review of the current NBI endoscopic classifications, so as to provide a useful guidance for precise diagnosis. We also present several possible advancements of other diseases which will be explored further. Moreover, we have proposed some improvements on the classification and diagnosis of several types of diseases, which are still currently under research. We present the following article in accordance with the Narrative Review reporting checklist (available at https://qims.amegroups.com/article/view/10.21037/qims-22-728/rc).

Methods

A systematic literature search was conducted in the PubMed database using the keywords "narrow band imaging", "NBI", and "classification". Articles published from 1 January 1994 to 10 November 2021 were included. Two investigators independently checked each identified article according to the inclusion criteria. A total of 75 English articles were selected. *Table 1* shows the detailed search strategy.

The mechanism of NBI

NBI is one of the advanced endoscopic imaging technologies. Since the first pilot study reported by Sano *et al.* in 2001, it has been applied for decades (18,19). NBI can improve the resolution and contrast of an image by using a superior method of visualizing the mucosal and submucosal vasculature (20). When the instrument is in NBI mode, the optical filters only allow 2 specific

wavelengths to pass through, namely, 415 nm (blue light) and 540 nm (green light). The blue light and green light are absorbed by hemoglobin (21). The wavelength of blue light is relatively short and can clearly detect the appearance of superficial mucosal vessels with brown color. In contrast, the green light can be used to show the appearance of the blood vessels in the submucosa with cyan color.

The application value of NBI in the detection of early cancer is that it can identify the intrapapillary capillary loops (IPCLs) (21-23). In stratified epithelium, IPCLs are single loops originating from the arborescent vascular network, which is connected to the submucosal vessels (24). The structure of the vessels changes dynamically to ensure metabolic exchanges. The IPCLs initially elongate and dilate, and when tumors invade the submucosa, they are destroyed and replaced by irregular neo-tumor vasculature (24,25).

NBI can therefore be used as a powerful tool to observe endoscopic features and make classifications for better diagnosis. As such, we will present literature reviews for the existing NBI classifications of different organs.

Head and neck tumors

NBI, to date, has been used in the diagnosis and classification of lesions located in the head and neck, including oral, pharyngeal, laryngeal, and sinonasal diseases. Using NBI, the surface and the capillaries can be seen clearly, and thus, classifications are always based on their morphology.

The classifications of laryngeal lesions

NBI is valuable in detecting early laryngeal cancer (26,27) and currently, 4 types of classifications are available, including Ni Classification 2011, Ni Classification 2019, the European Laryngological Society (ELS) Classification, and Puxeddu Classification (*Table 2*).

Ni Classification was initially reported in 2011, and updated in 2019 with an additional classification of the vocal cord leukoplakia. In Ni Classification 2011, Ni classified IPCL changes into 5 groups (I to V). Type I to IV are considered benign. Type V, which is regarded as malignant is subdivided into types Va, Vb, and Vc according to shape, regularity, and distribution of vessels (28).

In Ni Classification 2011, the vocal cord leukoplakia was assigned to type III lesions. However, different researchers have reached different conclusions when they observed the images. Therefore, Ni *et al.* updated the Ni Classification in 2019 to resolve the inconsistencies. The 2019 version

Table 1 Summary of the literature search strategy

Items	Specification
Date of search	Nov 10, 2021
Database and other sources searched	PubMed
Search terms used	"narrow band imaging", "NBI", and "classification"
Timeframe	January 1994 to November 2021
Inclusion and exclusion criteria	Inclusion criteria: articles which describe the classification of NBI
	Exclusion criteria: articles which describe the features of diseases but with no classification
Selection process	Z Liu and Q Yang conducted the selection, all authors attended a meeting to discuss the literature selection and a consensus was reached.

NBI, narrow-band imaging.

divided vocal cord leukoplakia into 6 types (*Figure 1*) (29).

ELS Classification was reported by Christoph Arens, and divides the vocal fold diseases into 2 groups, namely, benign and premalignant or malignant lesions. They specified that the benign conditions include longitudinal vascular changes, such as ectasia, meandering vessels, increasing number and density of blood vessels, and vessel branches or direction changes. However, indicator vessels are not specific a symptom of benign lesions as they can also occur in malignant lesions. Therefore, when clinicians observe this kind of change, they need to examine the pathology of the vocal fold. Moreover, the premalignant lesions are featured by perpendicular vascular changes, indicating dilated IPCLs. The spiral shape with wide-or narrow-angled turning points indicate recurrent respiratory papillomatosis (RRP) or precancerous or cancer lesions, and further attention is warranted when clinicians observe this change (30).

The Puxeddu Classification, developed by Puxeddu *et al.*, is used to detect neoangiogenesis in tumors. It is divided into 5 types (0 to IV) based on the enhanced contact endoscopy vascular patterns. Each type represents normal mucosa, inflammation, hyperplasia, mid-moderate dysplasia, and high-grade dysplasia (HGD)/carcinoma in situ (CIS)/ invasive carcinoma, respectively (31).

Some researchers have compared the previous 3 classifications, and set up a vocal fold leukoplakia (VFL) management algorithm (32). Indeed, a deeper understanding of these classifications may help clinicians to better manage diseases.

The classification of sinonasal lesions

Bruno *et al.* introduced the sinonasal mucosa (SN) patterns,

which are classified into five groups (SN1 to SN5), to assist the diagnosis of sinonasal diseases.

SN1 is regarded as the normal mucosa and the images vary along with the subsite of the nasal cavity: head of turbinate: a dotted pattern composed of small and close dark dots; body of turbinate: a simple network of loosely arborescent vessels oriented in a parallel manner and in posterior-anterior direction; and nasal septum: small and thin dark-blue vessels which are crowded and densely branched.

SN1 is only represented in normal mucosa, whereas SN2–5 can be observed in various diseases. SN2 represents the irregular speckles with a background of edematous mucosa; it shows diffuse and thin vessels compared to SN1, which can be found in allergic rhinitis, atrophic rhinitis, chronic rhinosinusitis without nasal polyps (CRSsNP), and normal mucosa.

The image of SN3 is green/blue oblique vessels sparsely distributed in a "broken apart" fashion, while an underlying vascular background is not clearly visible. SN3 can be found in sinonasal papilloma, eosinophilic granulomatosis with polyangiitis (formerly, Churg-Strauss syndrome), chronic rhinosinusitis with nasal polyps (CRSwNP), CRSwNP in cystic fibrosis, allergic rhinitis, synechiae, and squamous cell carcinoma.

SN4 is described as large elongating and congested vessels with thinner anastomoses joining the individual branches. It can be observed in different pathology pictures of sinonasal disease, including sinonasal papilloma, eosinophilic granulomatosis with polyangiitis, Schwannoma, intestinal-type adenocarcinoma (ITAC), septal perforation, CRSsNP, granulomatosis with polyangiitis (formerly, Wegener's granulomatosis), CRSwNP in cystic fibrosis,

Table 2 The classifications of laryngeal lesions

Classification	Lesion manifestations
Ni Classification [2011]	I: IPCLs are almost invisible, while oblique and arborescent vessels of small diameter can be seen
	II: IPCLs are almost invisible, but the vessels that can be seen have a larger diameter
	III: the mucosa is white and the IPCLs are invisible, and whether oblique and tree-like-vessels can be seen is dependent on the thickness of the white patch
	IV: mucosal IPCLs are arranged comparatively regularly and are low in density. There are bifurcations or slight dilations of the capillary terminals, and IPCLs appear to be scattered, tiny, dark brown spots. Oblique and arborescent vessels are usually invisible
	Va: with their high density and prominent dilation, IPCLs can appear solid or hollow, brownish, speckled, and shaped in various ways
	Vb: as IPCL destructs, its remnants look like snakes, earthworms, tadpoles, or branches. Additionally, the micro-vessels dilate, elongate, and appear woven
	Vc: necrotic tissue covers the lesion surface, and the tumor surface is irregularly covered with IPCLs which appear as brownish speckles or tortuous shapes with uneven density
Ni Classification of the vocal cord leukoplakia [2019]	I: in contrast to IPCLs, white plague is observed, with obliquely running vessels and branching vessels under it
	II: white patches appear, but IPCLs, obliquely running vessels, or branches cannot be seen
	III: on the surface of the vocal cord mucosa without leukoplakia, IPCLs appear as small brown spots with a relatively regular arrangement without boundaries. There are no obliquely running or branching vessels
	IV: IPCLs can be observed, showing large brown spots and embedded at the surface of white plaques
	V: IPCLs can be seen, shown as large brown spots, which appear at the surface of the vocal cord mucosa outside the leukoplakia with obvious boundaries
	VI: IPCLs are visible, characterized by large brown spots or twisted earthworm-like vessels distributed at the surface of the leukoplakia and also at the surface of the vocal cord epithelium outside the leukoplakia
ELS Classification [2016]	Benign lesions: longitudinal vascular changes
	Premalignant lesions: perpendicular vascular changes
Puxeddu Classification [2015]	0 (normal mucosa): thin-end regular subepithelial vessels connecting with a thicker and deeper arborescent vascular network running parallel to the epithelium
	I (inflammation): the subepithelial vessels are increased in number and size, with irregular and sometimes crossing directions.
	II (hyperplasia):
	(i) Initial stage: intra-CLs are visible running toward the surface. CLs are generally still very thin and short, arising from the underlying inflammatory vasculature, with a scattered distribution;
	(ii) Mature hyperplasia: the deeper inflammatory vascular network is not visible, and only the elongated CLs can be easily seen;
	(iii) Vegetating keratosis: the deeper inflammatory vascular network is often not visible, and the elongated CLs are difficult to see. A particular type of "bobby-pin" which is encased by typical papilloma can be seen in laryngeal papillomatosis.
	III (mild-moderate dysplasia): vascular changes become more consistent, with elongated small vessels in the typical "bobby-pin" shape, but some arborescence appears at the end of the CLs
	IV (high-grade dysplasia/carcinoma in situ/invasive carcinoma): the vascularity of the chorion is more evident, and CLs appear significantly dilated, with various shapes and a wide range of vascular architectural changes such as corkscrews or tree-like patterns

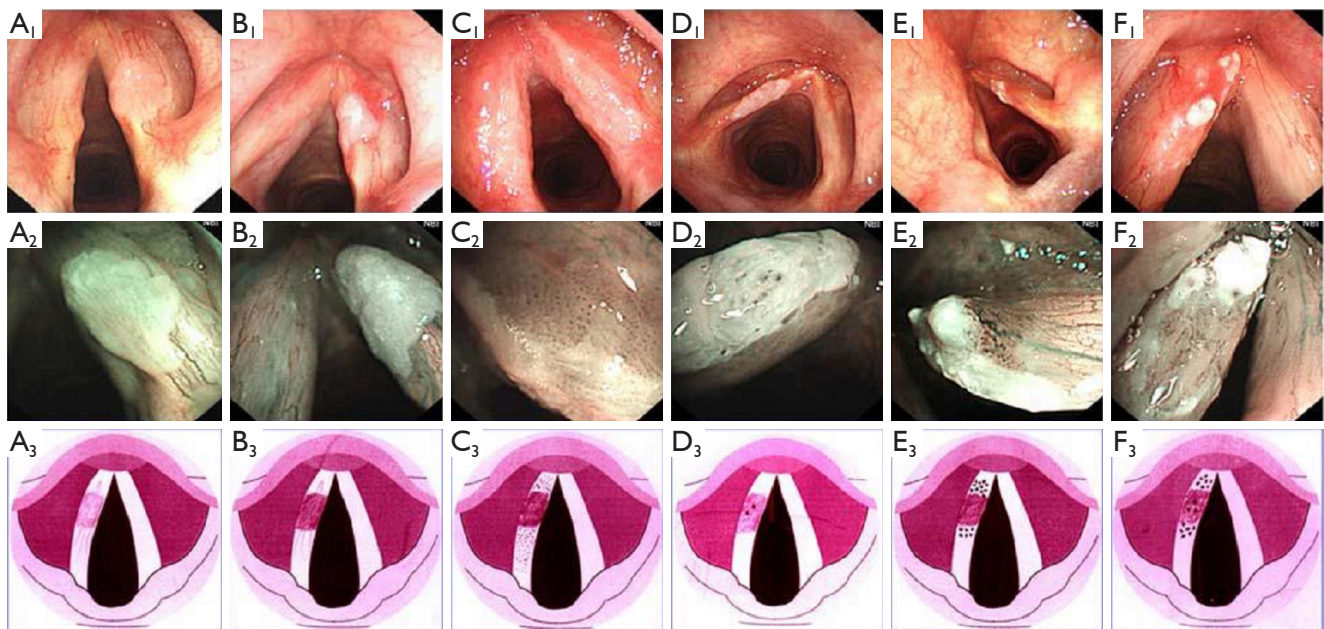IPCLs, intrapapillary capillary loops; CLs, capillary loops.

Figure 1 The Ni Classification 2019. Classification of vocal cord leukoplakia according to IPCL patterns. (A1-3) Type I IPCL pattern; (B1-3) type II IPCL pattern; (C1-3) type III IPCL pattern; (D1-3) type IV IPCL pattern; (E1-3) type V IPCL pattern; and (F1-3) type VI IPCL pattern. This figure is licensed by John Wiley and Sons. IPCL, intraepithelial papillary capillary loop.

plasmacytoma, mucosal melanoma, and synechiae.

In SN5, IPCLs are clearly visible with a relatively smooth arrangement. It often shows up in granulation, mucosal melanoma, ITAC, and squamous cell carcinoma (33).

The classifications of pharyngeal lesions

NBI is highly powerful, not only in differentiating nonmalignant from malignant lesions (34), but also in detecting precancerous lesions and predicting the invasive depth and thickness of pharyngeal tumors (35-37). To date, the classifications include IPCL Pattern Classification, namely, the Japan Esophageal Society Classification (JES Classification), and the NBI Classification of nasopharyngeal mucosal microvessel patterns.

The squamous epithelium which covers the pharynx is the same as the one on the esophagus. The invasive depth can be determined based on the pattern of the IPCLs, as detected by magnifying endoscopy with narrow-band imaging (ME-NBI) (38). Therefore, the classification criteria for these vascular patterns, such as IPCL Pattern Classification and JES Classification, can also be applied in the differentiation of pharyngeal diseases. In contrast, the JES Classification is used more frequently in routine practice. These 2 classifications will be described as part of esophageal diseases.

The Ni Classification has been used for the early diagnosis of head and neck squamous cell carcinomas (HNSCCs) and this classification also shares some common criteria with the JES Classification. Eguchi found that Va and Vb of the Ni Classification corresponded to the B1 and B2 Classification, respectively (28,36,39-41).

Ni *et al.* introduced the NBI Classification of nasopharyngeal mucosal microvessel patterns, which can be classified into the following 5 types (I to V) based on the morphology of the IPCL (*Table 3*). They also studied the relationship between histopathological diagnosis and endoscopic findings. The conclusion was that normal nasopharyngeal mucosa showed as type I, lymphoid hyperplasia often appeared as type II, nasopharyngeal radiation-induced inflammation showed as type III or IV, and nasopharyngeal carcinoma (NPC) mainly exhibited type V (42).

The classifications of oral lesions

Takano summarized a new IPCL classification of oral mucosa on the basis of Inoue's classification (40), and

Table 3 NBI classification of nasopharyngeal mucosal microvessel patterns

Type	IPCLs	Microvascular network	The submucosal veins
Type I	Invisible	Oblique and arborescent vessels and can be observed as thin, short brownish line shapes	Indistinct, dark-green stump shapes
Type II	Invisible	Oblique and arborescent vessels can be observed indistinctly and nearly disappear	Invisible
Type III	Invisible	Oblique and arborescent vessels which are engorged and can be seen clearly as fine brownish lines	Enlarged and can be seen clearly as thick, twisted, dark-green line shapes
Type IV	Visible, with a relatively regular arrangement and high density, appear as scattered, small, dark-brown dots.	Nearly invisible	Nearly invisible
Type V	Dilated, elongated, and distorted, and appear clearly as irregular, twisted, brownish line shapes; have snake-like, earthworm-like, or branch-like shapes.	Nearly invisible	Nearly invisible

NBI, narrow-band imaging; IPCLs, Intrapapillary capillary loops.

divided it into 4 types (I to IV). The morphology of the IPCL varies in each type.

Type I appears as a waved line with both waved arms. Type II is dilated and is similar to type I, but has a much larger caliber than those far from the lesion. Type III displays generally elongated IPCLs that are accompanied by dilation. They can appear as long lines or as tangled lines due to a severe increase in length. Type IV is in the progression of carcinogenesis, the terminal branch loops dilate, elongate, and eventually destruct. Considering the histology, type I occurs in the normal mucosa, types II and III occur in non-neoplastic lesions with predominance of the latter, and types III and IV occur in neoplastic lesions (15).

Although previous studies have only focused on the histology, Tirelli holds a different opinion. He suggested that it is necessary to consider the different epithelial structures (43,44). On the basis of both the epithelial structure in the different oral subsites and the different tissue, he proposed the following 6 vascular patterns on NBI: normal 1, 2a, 2b, dysplastic 1–2a, and 2b. The appearance of malignant lesions was also described (*Figure 2*).

The classification of the epithelium was raised by Lin *et al.* in 2012, which helps us understand why different sites of the same organ show different images. In this classification, 4 types of epithelia were described, including type 1 or keratinized thick stratified squamous; type 2a or nonkeratinized thin stratified squamous; type 2b or nonkeratinized very thick stratified squamous; and type 3 or pseudo-stratified ciliated columnar epithelium (44) (*Table 4*).

Upper gastrointestinal lesions

The first pilot study by Sano *et al.* showed that NBI can be used to diagnose gastric, esophageal, and colorectal lesions by examining the surface structure and capillaries (18). A large number of studies have since been published regarding NBI (45-52) and several classifications have been developed for the diagnosis of various lesions.

The classifications of esophageal lesions

Superficial esophageal squamous cell carcinoma

Microvascular (MV) patterns of IPCLs, first identified under white light, were up until recently, the only reliable indicator of tissue atypia (22,53). Later, research demonstrated that NBI can detect superficial cancer more frequently than white light imaging in the esophagus, since it can better recognize IPCLs. Based on these findings, the IPCL classifications were first established in 2001 and continue to be updated. This 5-tier classification (type 1 to 5) is well-matched to histological characterization with normal tissue, esophagitis, mild dysplasia, severe dysplasia, and cancer (54).

Considering the clinical relevance and convenience of reference to the general user, a novel categorization of the original IPCL classification was put forward in 2015. In this classification, the categories of IPCL classification
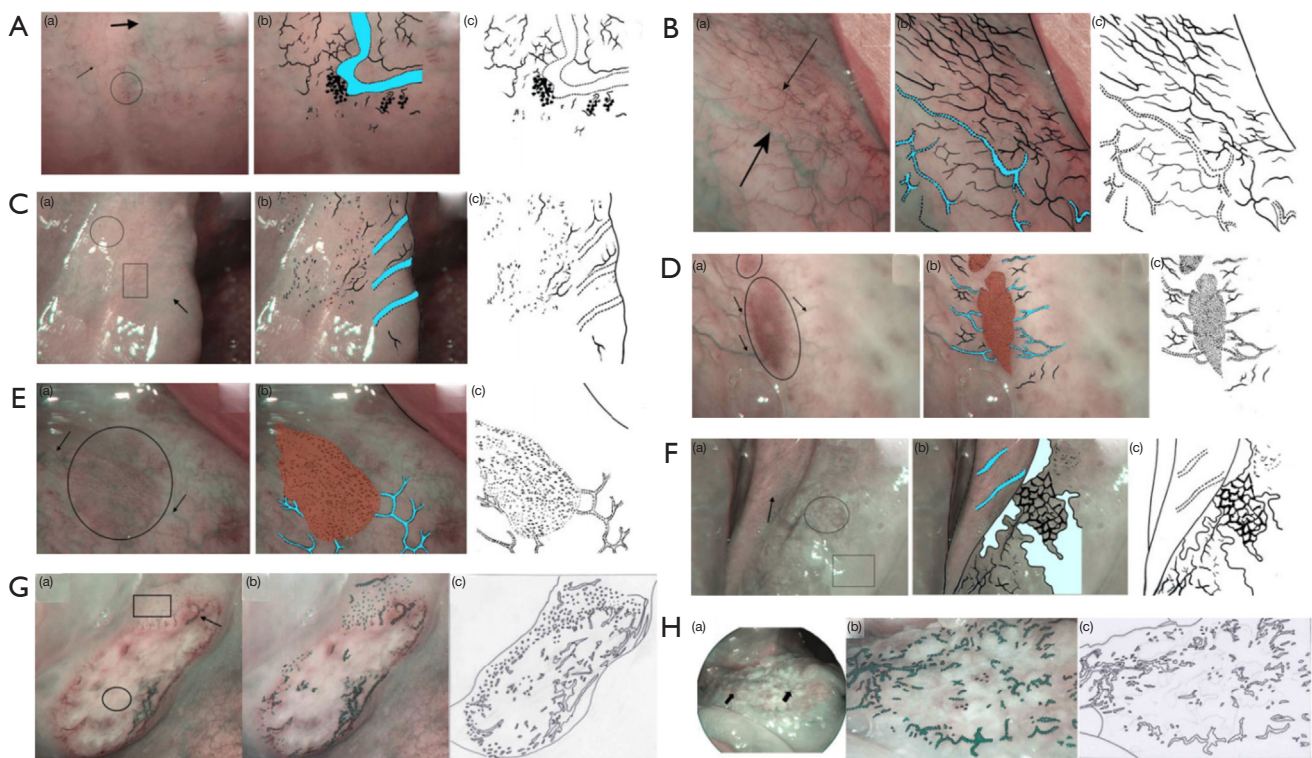
Figure 2 The classification raised by Tirelli. (A) Normal pattern in type 1 epithelium: (a) posterior hard palate appearance on NBI endoscopy. Superficial mucosal capillaries (thin arrow), submucosal veins (thick arrow), and flower-like structures (circle); (b) superficial mucosal capillaries, submucosal veins (in cyan), and flower-like structures; (c) schematic drawing. (B) Normal pattern in type 2a epithelium: (a) floor of mouth appearance on NBI endoscopy. Superficial mucosal capillaries (thin arrow), submucosal veins (thick arrow); (b) superficial mucosal capillaries and submucosal veins (in cyan); (c) schematic drawing. (C) Normal pattern in type 2b epithelium: (a) inferior trigone appearance on NBI endoscopy. Superficial mucosal capillaries (circle, rectangle), submucosal veins (arrow); (b) superficial mucosal capillaries and submucosal veins (in cyan); (c) schematic drawing. (D) Dysplastic pattern in type 1 epithelium: (a) severe dysplasia of the hard palate on NBI endoscopy. A well-demarcated brownish/purple area with thick dark spots is visible (circle); it is perpendicularly reached by dilated light blue vessels (arrows); (b) the well-demarcated brownish/purple area perpendicularly reached by dilated light blue vessels (in cyan); (c) schematic drawing. (E) Dysplastic pattern in type 2a epithelium: (a) severe dysplasia of the floor of mouth on NBI endoscopy. A well-demarcated brownish/purple area with thick dark spots is visible (circle); it is perpendicularly reached by dilated light blue vessels (arrows); (b) the well-demarcated brownish/purple area perpendicularly reached by dilated light blue vessels (in cyan); (c) schematic drawing. (F) Dysplastic pattern in type 2b epithelium: (a) severe dysplasia of an inferior trigone on NBI endoscopy. Mesh (circle), leukoplakia (rectangle) and the submucosal vessels (arrow); (b) the image resembles a mesh, leukoplakia, and the submucosal vessels (in cyan); (c) schematic drawing. (G) Neoplastic pattern in an ulcerated cancerous lesion: (a) ulcerated cancer of the hard palate on NBI endoscopy. Necrosis in the center of the lesion (circle), dark green spots (rectangle), dilated winding vessels or bobby-pin (arrow); (b) dark green spots, dilated winding vessels, or bobby-pin; (c) schematic drawing. (H) Neoplastic pattern in a vegetating cancerous lesion: (a) vegetating cancer of the floor of mouth on NBI. Unstructured vessels appearing as dark green spots, dilated winding vessels or as bobby-pin (arrow); (b) dark green spots, dilated winding vessels, or bobby-pin; (c) schematic drawing. This figure is licensed by John Wiley and Sons. NBI, narrow-band imaging.

were redistributed into 3 groups: Group 1 (non-neoplastic: IPCL I and II), Group 2 (borderline: IPCL III and IV), and Group 3 (cancer: IPCL V) (14).

In 2005, Arima *et al.* also put forward an endoscopy classification of MV patterns (types 1 to 4) to help diagnose

and assess the extent and depth of tumor invasion (55). However, this study was conducted with magnifying endoscopy (ME), namely optical magnifying video endoscope.

For the sake of convenience and efficacy, researchers used

Table 4 Vascular patterns and corresponding epithelium classification on NBI of oral lesions

Type	Morphology	The type of epithelium
Normal 1	Superficial mucosal capillaries: thin dark green/brown vessels with small branches arising at an acute angle in the posterior hard palate, punctuations along the palatine crests in the anterior-lateral part of the hard palate and mucosa of gingiva	Type1 epithelium
	Submucosal veins: some large light blue vessels could be glimpsed	
	Minor salivary glands: some of the branching vessels ended with a "flower-like" configuration with a thin vessel acting as a "stem" and several points all around as the "petals"	
Normal 2a	Superficial mucosal capillaries: thin dark green/brown vessels with small branches arising at an acute angle	Type2a epithelium
	Submucosal veins: large light blue vessels were clearly visible	
Normal 2b	Superficial mucosal capillaries: regular and equidistant dark green/brown small punctuations or short dashes if the vessels were visualized perpendicularly, or thin parallel vessels if they were longitudinal to the mucosa	Type2b epithelium
	Submucosal veins: some large light blue vessels could be glimpsed	
Dysplastic 1–2a	Mucosa: a well-demarcated brownish/purple area with thick dark spots	Type1 and 2a epithelia
	Submucosal veins: large light blue vessels are invisible in the brownish/purple area, and the dilated light blue vessels can perpendicularly reach the lesion	
Dysplastic 2b	Mucosa: a honeycomb mesh made up of multiple polygonal areas. Submucosal veins: large light blue vessels are invisible, but can sometimes be seen in the surrounding areas	Type 2b
Neoplastic	Dark green spots, dilated winding vessels or a bobby-pin can be seen over the whole cancer surface, in the case of ulcerated lesions, the presence of a necrotic core prevents visualization of the vasculature	–

NBI, narrow-band imaging.

ME-NBI to integrate the classifications mentioned above into 1 simplified classification, the JES Classification (56). The JES Classification system consists of the following 2 types: type A microvessels are associated with noncancerous lesions and lack severe irregularity, whereas type B microvessels are associated with cancerous lesions with severe irregularity. According to the indications for endoscopic resection (ER), type B vessels can be subdivided into B1, B2, and B3, which correspond to an absolute indication type, a relative indication type, and a contraindication type, respectively.

As for the morphology, type A was described as normal IPCL or abnormal microvessels without severe irregularity. The characteristic of type B is abnormal microvessels with severe irregularity or highly dilated abnormal vessels. B1 is defined as type B vessels with a loop-like formation with dot-like microvessels. B2 is defined as type B vessels without a loop-like formation, a stretched and markedly elongated transformation with a multilayered arrangement or an irregularly branched/running pattern are typical feature. B3 is defined as highly dilated abnormal vessels appearing

green in color. In addition, the diameter of B3 is 3 times more than that of the B2 vessels.

Barrett's esophagus (BE)

NBI is a promising tool for identifying specialized intestinal metaplasia (SIM), dysplasia, and early cancer in patients with BE. Moreover, it has been shown to accurately diagnose disease according to histology findings (57-63).

On the basis of correlation with histology, in 2006, Sharma *et al.* established the Classification of mucosal and vascular patterns according to NBI endoscopy. Also known as the Kansas Classification, it describes 3 specific mucosal patterns and 2 distinct vascular patterns (59).

In the same year, Kara *et al.* noted the mucosal morphology and vascular patterns and recommended a hierarchical classification and a risk stratification of mucosal morphology, called the Amsterdam Classification (58).

Since the first 2 preliminary descriptive studies showed a strong correlation between NBI findings and histology, investigators moved to validate a simplified mucosal

morphology classification called Nottingham Classification in 2008. Singh *et al.* (60) classified the mucosal morphology into 4 types (type A to D): columnar mucosa without intestinal metaplasia, intestinal metaplasia, low-grade dysplasia (LGD), and HGD in BE.

To further validate the 3 classifications, a specific study was performed. It was found that the 3 classifications could be used in the clinical environment. However, there was no adequate interobserver agreement (64). In addition, due to the complexity involved, a simplified classification of mucosal morphology merely focusing on capillary pattern (CP) was established in 2015, namely, the Classification of Capillary and Pit Pattern (CP Classification) (65). This classification categorized the images into 2 types: type I and type II.

Prior to the introduction of CP Classification, there was another classification which also referred to the morphology of mucosa and vessels. Anagnostopoulos *et al.* used high resolution magnification endoscopy (HRME) and NBI to identify SIM and dysplasia in BE in 2007 (66) (*Figure 3A,3B*).

Until 2015, none of the classifications mentioned above were accepted widely. Therefore, Barrett's International NBI Group (BING) developed a consensus-driven NBI Classification called the BING Criteria. It was aimed at helping clinicians better identify intestinal metaplasia/nondysplastic Barrett's esophagus (NDBE) and HGD/esophageal adenocarcinoma (EAC) (67). According to this classification, mucosal and vascular patterns are both categorized as regular or irregular.

Additionally, the JES also developed a consensus-based and more simplified classification in 2018, called the JES-BE classification. It was used to recognize superficial BE-related neoplasms with high-definition magnification NBI (HM-NBI). Compared with other classifications, this was easy to understand by integrating the diagnostic criteria for early gastric cancer with novel diagnostic criteria, resulting in a modified flat pattern corresponding to non-dysplastic histology (39).

The mucosal morphology in the classification systems mentioned above is described in *Table 5*.

The classifications of gastric lesions

Yao *et al.* performed a series of studies for the diagnosis of gastric lesions based on MV architecture and density (68-70). In 2009, they established the Yao vessel plus surface (VS) Classification System which is based on MV patterns and microsurface (MS) patterns. Both of these consist of 3 types of manifestations: regular, irregular, and absent. Yao *et al.* also described the hallmarks of early gastric cancer, which is an irregular MV pattern and/or an irregular MS pattern together with a clear demarcation line (71).

The classification raised by Nakayoshi *et al.* was based on classifying the MV patterns into the following 3 groups: A, fine-network pattern (FNP); B, corkscrew pattern (CSP); and C, unclassified pattern which was not mentioned concretely in the previous research (72). However, Yokoyama *et al.* held the opinion that neither FNP nor CSP are applicable to early gastric lesions. As such, they further worked on an unclear pattern which is described as 'unclassified pattern' in the classification raised by Nakayoshi *et al.*, leading to the definition of a new category, the intra-lobular loop pattern (ILL). They also raised a novel classification based on abnormal MV pattern and irregularity of superficial glandular structure which divided the NBI images into 4 categories: FNP, ILL-1, ILL-2, and CSP. They concluded that differentiated-type of adenocarcinomas show abundant vascular patterns, such as "FNP" or "ILL"; whereas the undifferentiated-type of adenocarcinomas show poor vascular patterns, for example, "CSP" or "ILL-2" (73). These classifications were similar those outlined in the study by Inoue *et al.* (74).

To classify gastrointestinal superficial neoplastic lesions and predict the presence of submucosal invasion, the Paris Classification, which is based on white light, was put forward in 2002. This is an international standard classification, developed from the Japanese macroscopic classification for gastric cancer (75,76). The classification divided the lesions into 3 categories: protruding lesions, non-protruding lesions, and excavated lesions. Each of them can be subdivided with different occurrence. Several studies were performed to differentiate between adenomas (ADs) (Vienna classification category 3) and carcinomas (Vienna classification category 4 or 5) (77-79), as both belonged to 0–II lesions according to the Paris classification (80). However, there remain several difficulties in distinguishing between ADs and carcinomas through evaluating the vascular patterns of lesions. Nakamura *et al.* established another classification on the basis of superficial structures (SSs) and irregular microvascular patterns (IMVPs) (81). Subsequently, Kobayashi *et al.* established A–B classification which is useful for differentiating gastric carcinomas from ADs (82). They found that A type and AB type lesions were associated with carcinomas, whereas B type lesions were ADs and carcinomas.

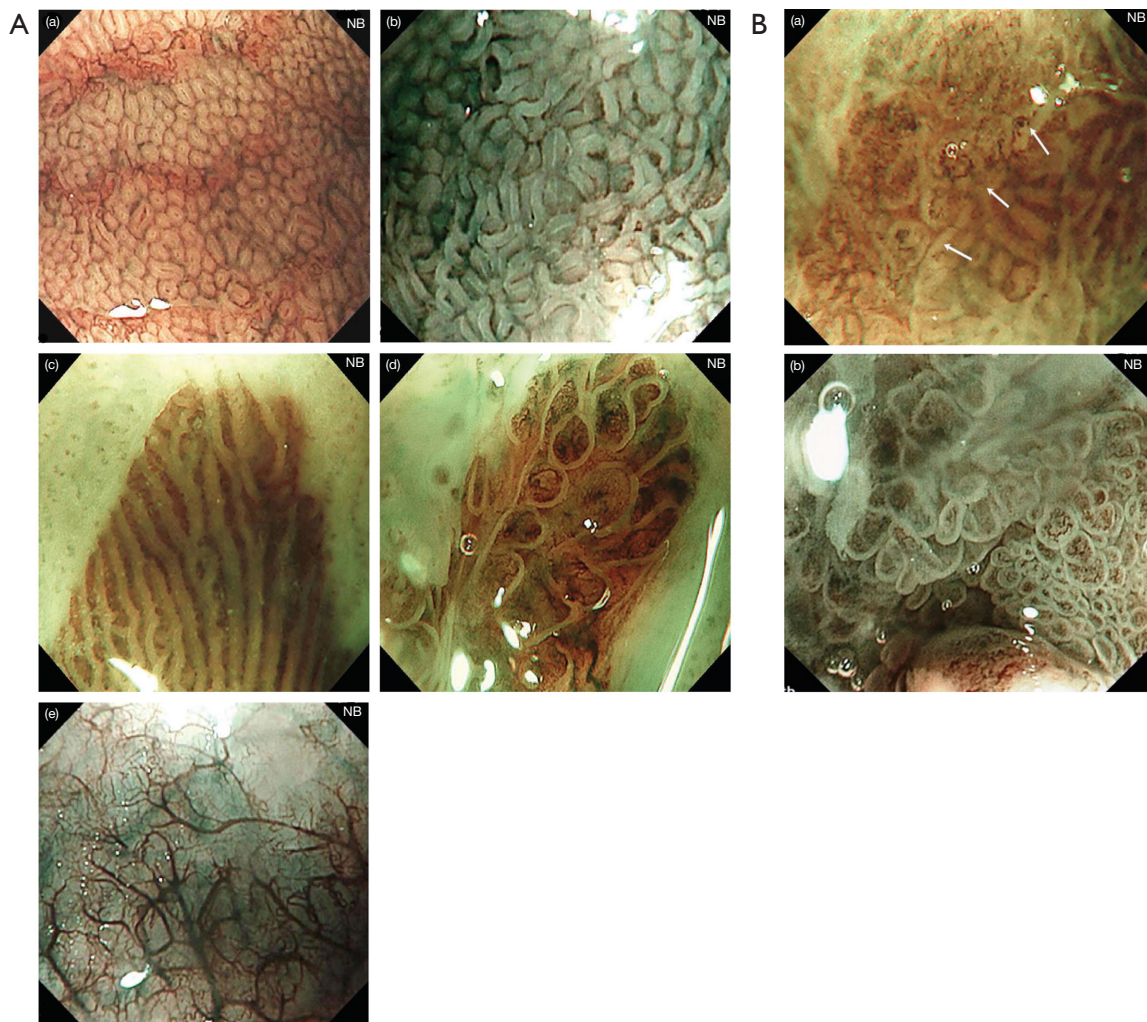In addition, due to the inconsistent reliability and

Figure 3 High resolution magnification endoscopy plus NBI findings of Barrett's epithelium. (A) Narrow-band endoscopic imaging of in non-dysplastic Barrett's esophagus shows microstructural and microvascular changes: (a) RMSP with round pattern; (b) RMSP with tubular pattern; (c) RMSP with linear pattern, (d) RMSP with villous pattern; (e) absent microstructural pattern. (B) Narrow-band endoscopic imaging of in neoplastic Barrett's esophagus shows microstructural and microvascular changes: (a) figure shows a clear demarcation line (white arrows) between the neoplastic mucosa with irregular microvessels (left part) and the non-neoplastic mucosa with regular microstructural pattern (right part); (b) figure shows IMSP with irregular microvascular pattern. This figure is licensed by John Wiley and Sons. NBI, narrow-band imaging; IMSP, irregular microstructural pattern; RMSP, regular microstructural pattern.

external validity of NBI in the stomach, Pimentel-Nunes *et al.* proposed a simplified classification. This classification was associated with the different patterns and different histology conditions: "regular vessels with circular mucosa" (pattern A), "tubulo-villous mucosa" (pattern B), and "irregular vessels and mucosa" (pattern C). The 3 types are associated with normal histology, intestinal metaplasia, and dysplasia, respectively (83).

The classifications of duodenal lesions

Ampullary tumors

In 2006, Uchiyama *et al.* attempted to establish a classification with ME-NBI to differentiate benign and malignant ampullary tumors based on the vessel patterns and surface structures of the ampullary lesions (84). They classified the images into 3 groups: I, oval-shaped

Table 5 NBI classification systems of Barrett's esophagus

Classification system	Manifestation
Amsterdam Classification	Mucosal pattern: regular (flat, villous/gyrus, other), irregular/disrupted
	Vascular pattern: regular, irregular, normal-appearing long branching vessels
Kansas Classification	Mucosal pattern: ridge/villous, circular, irregular/distorted
	Vascular pattern: normal (presence of thin vessels with a uniform branching pattern), abnormal (dilated, corkscrew vessels with increased vascularity and abnormal, non-uniform branching pattern)
Anagnostopoulos' Classification	Mucosal pattern: regular microstructural pattern, irregular microstructural pattern, absent microstructural pattern
	Vascular pattern: regular microvascular pattern, irregular microvascular pattern
Barrett's International NBI Group (BING) Criteria	Mucosal pattern: regular (circular, ridged/villous, tubular), absent, irregular
	Vascular pattern: regular (blood vessels situated regularly along or between mucosal ridges and/or those showing normal, long, branching patterns), irregular (focally or diffusely distributed vessels not following normal architecture of the mucosa)
Japan Esophageal Society Barrett's esophagus (JES-BE) Classification	Mucosal pattern: invisible (flat), visible (pit, non-pit)
	Vascular pattern: invisible (flat), visible (net, non-net)
Nottingham Classification	Type A: round pits with regular microvasculature
	Type B: villous/ridge pits with regular microvasculature
	Type C: absent pits with regular microvasculature
	Type D: distorted pits with irregular microvasculature
Classification of Capillary and Pit Pattern (CP Classification)	Type I: uniform branches or vine-like pattern with a clear shape that can be traced smoothly
	Type II: coiled or spiral pattern with a nonuniform shape that cannot be traced sufficiently and with increased vascularity

NBI, narrow-band imaging.

villi; II, pinecone/leaf-shaped villi; and III, irregular/nonstructured. In addition, they also set up the definition of abnormal vessels: dilated, tortuous, or network-like vessels. By integration of the observation and histological confirmation, they found that type I surface structure occurred in inflammation or hyperplastic lesions, whereas type II and/or III occurred in ADs and adenocarcinomas. Additionally, they can be used to differentiate ampullary ADs from adenocarcinomas since abnormal vessels only appear in adenocarcinomas. However, the limitation of this study is that there were only a few cases, which indicates that further studies are still needed.

Until 2015, Park *et al.* put forward 4 types of meaningful irregular villous patterns: irregular villous arrangement, irregular villous size, disappearance of ridge, and demarcation with normal villi. Abnormal microvasculature was defined as dotted or significantly dilated vessels. Through multivariate analysis, they concluded that ampullary tumors (adenoma and adenocarcinoma) had irregular villous arrangement and abnormal microvasculature. Unlike previous research, abnormal microvasculature was the only significant factor associated with adenoma but not adenocarcinoma. As for the other types, it was not used for tumor identification (85).

Non-ampullary duodenal lesions
Recently, it has been confirmed that NBI can be used in the detection of non-ampullary duodenal tumors (86-88). Accordingly, several classifications were proposed.

In 2014, Kikuchi *et al.* developed a classification focusing on surface pattern and vascular patterns with ME-NBI in order to detect superficial non-ampullary duodenal epithelial tumors (SNADETs) (89). They also discovered the relationship between the patterns and pathology according to the revised Vienna classification (90): all

mixed-type lesions correlated with category 4/5 tumors; monotype lesions, absent pattern, and network pattern lesions correlated with category 3 tumors; unclassified pattern lesions correlated with category 4 tumors; and further validation is needed for intrastructural vascular (ISV) pattern lesions.

In 2015, Tsuji *et al.* used the VS classification system to detect early gastric cancer to evaluate SNADETs (71,91). They found that an irregular MS pattern is more frequent in Category 4, whereas a MV pattern shows no prominent difference between category 3 and category 4.

In 2017, Mizumoto *et al.* further enriched the Hiroshima classification, which is used to detect colic lesions to classify non-ampullary duodenal tumors. It revealed the relationship between NBI findings (type B or C) and Vienna classification (category 3 or 4) (90,92). Category 4 lesions are larger than category 3 lesions, and in category 4, type C lesions are more common than type B lesions (93).

Additionally, in 2019, Kakushima *et al.* reconsidered the limitations which existed in previous studies. The ME-NBI patterns were applied to differentiate low-grade adenoma (Vienna category 3, C3) and high-grade adenoma/carcinoma (C4/5) among SNADETs (88,89,91,94). Considering the surface structure and vasculature, 4 ME-NBI patterns were categorized: surface villous structure with intrastructural vessels; surface tubular structure with network vessels (network); surface villous structure with white opaque substance (WOS); and surface disappeared structure with irregular vessels (disappeared-irregular). It revealed that disappeared pattern should be considered as a specific feature to detect category 4/5 lesions. Some findings supported previous research by Kikuchi *et al.*, namely, that WOS is similar to a monotype of surface pattern suggestive of category 3, and disappeared-irregular is similar to a monotype of surface pattern with vascular unclassified patten (89).

Lower gastrointestinal lesions

Colorectal lesions

Many studies have suggested that NBI plays an important role in the diagnosis of colorectal lesions (95-97). As such, many researchers have made great efforts to simplify and unify the classifications.

In 2011, Tanaka *et al.* summarized the classifications of early gastric carcinoma (98), such as the Sano classification (99) (*Figure 4A*), Hiroshima classification (100,101) (*Figure 4B*), Showa classification (102) (*Figure 4C*),

vascular/surface classification (71), evaluation method of Kurume University, and the evaluation method of the Cancer Institute Hospital of Japanese Foundation for Cancer Research. Afterwards, they established an international classification called the Narrow Band Imaging International Colorectal Endoscopic (NICE) classification. Validation studies of NICE classification have shown that this classification is useful in diagnosis of colorectal lesions (103,104).

The pit pattern mentioned in the table was created by Kudo *et al.* Although it was not applied with NBI, it still plays an important role in the diagnosis of colorectal lesions (105,106). In 2007, Hirata *et al.* concluded that NBI magnification is useful for the assessment of pit patterns even without chromoendoscopy (107). However, in 2013, Hayashi *et al.* studied the relationship between NBI magnifying observation using Hiroshima classification and pit pattern for the diagnosis of colorectal tumors (108). They found that the effects of both methods were similar in detecting lesions with regular structure, whereas the pit pattern diagnosis was more detailed than NBI magnifying observation in lesions with irregular structures.

Although the classifications mentioned above have been reported useful in detecting colorectal lesions, there are still some clinical problems that cannot be resolved. Therefore, the Japan NBI Expert Team (JNET) classification was developed in 2016 by integrating 4 precious magnifying NBI classifications (the Sano, Hiroshima, Showa, and Jikei classifications). Based on vessel pattern and surface pattern, the endoscopic images can be divided into 3 types: type 1, type 2A, type 2B, and type 3 (109,110) (*Figure 5*). In the same year, considering that current classifications did not include neoplastic sessile serrated adenomas/polyps (SSA/Ps), the Workgroup Serrated Polyps and Polyposis (WASP) classification was proposed (111). This classification combined both NICE classification and criteria for differentiation of SSA/Ps, namely, the Hazewinkel criteria, to differentiate ADs, hyperplastic polyps (HPs), and SSA/Ps in a stepwise method (112).

In 2017, Sumimoto *et al.* evaluated the diagnostic ability of each type of JNET classification, and found that type 2B was the unreliable one. Thus, they proposed JNET classification and type 2B sub classification to improve the diagnostic performance and to choose better treatment methods (113). Type 2B was further divided into type 2B-low and type 2B-high according to the level of irregularity in surface and vessel patterns. The vessel pattern of type 2B-low is that the thickness and distribution
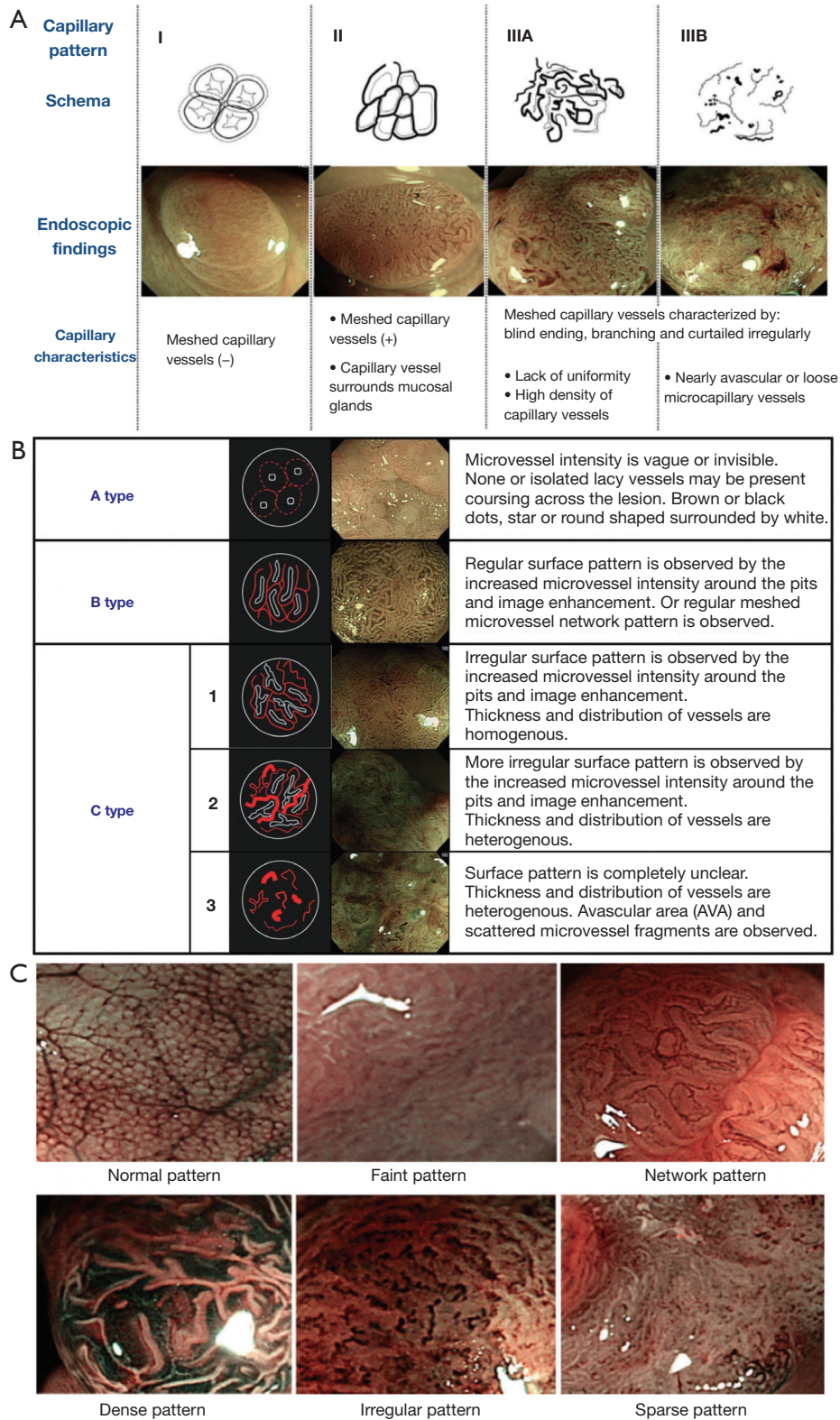
Figure 4 NBI magnifying observation classification proposed in Japan. (A) Sano classification. (B) Hiroshima classification. (C) Showa classification. This figure is licensed by John Wiley and Sons. NBI, narrow-band imaging.
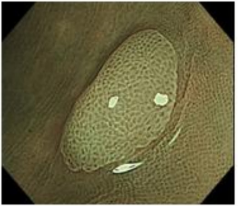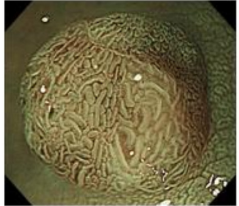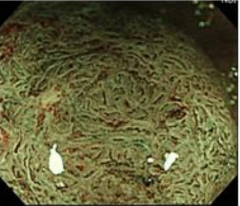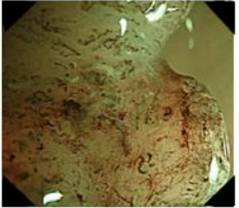
	Type 1	Type 2A	Type 2B	Type 3
Vessel pattern	• Invisible*1	• Regular caliber • Regular distribution (meshed/spiral pattern)*2	• Variable caliber • Irregular distribution	• Loose vessel areas • Interruption of thick vessels
Surface pattern	• Regular dark or white spots • Similar to surrounding normal mucosa	• Regular (tubular/branched/papillary)	• Irregular or obscure	• Amorphous areas
Most likely histology	Hyperplastic polyp/ Sessile serrated polyp	Low grade intramucosal neoplasia	High grade intramucosal neoplasia/Shallow submucosal invasive cancer*3	Deep submucosal invasive cancer
Endoscopic image				

Figure 5 The Japan NBI Expert Team classification. *1, if visible, the caliber in the lesion is similar to surrounding normal mucosa; *2, microvessels are often distributed in a punctate pattern and well-ordered reticular or spiral vessels may not be observed in depressed lesions; *3, deep submucosal invasive cancer may be included. This figure is licensed by John Wiley and Sons. NBI, narrow-band imaging.

of irregular vessels are uniform, whereas type 2B-high is the diameter and/or distribution of irregular vessels are heterogeneous. As for the surface pattern, the characteristics of type 2B-low are as follows: (I) irregular in the pit-like pattern net-work; and (II) smooth pit-like structure margin without ravaging. The characteristics of type 2B-high are: (I) irregular and destroyed pit-like pattern; and (II) irregular, fluffing, and unclear pit-like structure margins. They found that type 2B-low can be considered a reliable indicator for ER, since a large majority were LGD, HGD, superficial submucosal invasive (SM-s) carcinoma. As for type 2B-high, further examination is needed to differentiate HGD and SM-s carcinoma from deep submucosal invasive (SM-d) carcinoma. Similarly, Kobayashi *et al.* also thought that if the lesion is diagnosed as JNET type 2B, it needed further evaluation. Instead of proposing a sub-classification, they used pit pattern as an additional method (12) (*Table 6*).

Pancreatic lesions

Before NBI was applied in the diagnosis of mucin-producing tumor of the pancreas (MPTP), namely, intraductal papillary-mucinous neoplasm (IPMN), many researchers tried to classify the pancreatic lesions according to observations.

In 2000, Yamaguchi *et al.* classified the lesions based on the morphology and the inner color (114). The morphology was divided into 4 types: sessile, semipedunculated, villous, and vegetative tumors. The inner color can be divided into 2 types: white and red; and the red color can be observed as spotty or linear. However, this classification can only be used for pancreas mucinous lesions. In 2010, Miura *et al.* used this classification to categorize the images and found that NBI played an important role in the diagnosis of various lesions (115). Additionally, NBI can also be applied to the diagnosis of indeterminate pancreaticobiliary disease combined with per-oral video cholangiopancreatoscopy (116). They described 9 types of images: tortuous/dilated vessels, infiltrative stricture, polypoid mass, fish-egg lesion, vegetative mass, ulceration, low-papillary mucosal lesion, and finger-like villiform lesion. The former 4 types were significantly associated with neoplasia.

Gynecologic lesions

The classifications of endometriotic lesions

NBI has been reported to be useful in detecting small endometriotic lesions (117,118). Several researchers made

Table 6 NBI classification methods of colorectal lesions

Classifications	Evaluation method	Types
Sano classification	Capillary pattern	Type: meshed capillary vessels (–)
		Type II: meshed capillary vessels (+); capillary vessel surrounds mucosal glands
		Type III: occurs in deep SM invasive carcinomas
		Type IIIA: lake of uniformity; high density of capillary vessels
		Type IIIB: nearly avascular or loose micro-capillary vessels
Hiroshima classification	The pit pattern and microvessel features	Type A: normal or discolored lesion with invisible microvessels
		Type B: colorectal tumors with clear and regular pit-like pattern or regular meshed capillary network surrounding a pit
		Type C (C1–C3): colorectal tumors with unclear pit-like pattern, with avascular areas, and interspersed with irregular microvessels or fractured microvessels
Showa classification	Pit-like pattern and microvascular architecture	Normal pattern
		Faint pattern: the microvessels surrounding the pit are difficult to identify
		Network pattern: in tubular or tubulovillous adenomas
		Dense pattern: tubular adenoma
		Irregular pattern: deep SM invasive carcinoma
		Sparse pattern: deep SM invasive carcinoma
Jikei classification	Microvascular architecture and partially pit-like pattern	Type 1: vascular flow cannot be recognized
		Type 2: vascular diameter increases slightly
		Type 3: vascular diameter increases remarkably:
		3V: regular vessel stream
		3I: irregular vessel stream
		Type 4: microvessels are sparsely distributed
Evaluation method of the Fukuoka University Chikushi Hospital	Microvascular architecture and surface structure	Irregular: heterogeneous diversified and asymmetric
		Regular: homogeneous and symmetric
Evaluation method of the Cancer Institute Hospital of Japanese Foundation for Cancer Research	Microvessel pattern	Unclear: microvessels are uncertain
		Regular: microvessels on the tumor surface form a network
		Irregular: microvessels on the tumor surface don't form a network
Narrow band imaging international colorectal endoscopic (NICE) classification	Color; vessels; surface pattern	Type 1: Color: same or lighter than background. Vessels: None, or isolated lacy vessels might be present coursing across the lesion. Surface pattern: dark or white spots of uniform size, or homogenous absence of pattern. Most likely pathology: hyperplastic
		Type 2: Color: browner relative to background (verify color arises from vessels). Vessels: thick brown vessels surrounding white structures. Surface pattern: oval, tubular or branched white structures surrounded by brown vessels. Most likely pathology: adenoma
		Type 3: Color: brown to dark brown relative to background; sometimes patchy whiter areas. Vessels: has area(s) with markedly distorted or missing vessels. Surface pattern: areas of distortion or absence of pattern. Most likely pathology: deep SM invasive cancer

NBI, narrow-band imaging; SM, submucosal.

Table 7 Cicinelli classification

Types	Characteristics
Normal proliferative endometrium	Flat endometrial mucosa with no evident vascular network
Polyp	New growth with a vascular axis
Atrophic polyp	new growth with vascular axis and subtle regular vascular network
Myoma	A regular branching of vessels on a whitish surface
Chronic endometritis	Inhomogeneous endometrium, blue, green, or brown colored depending on vascularization characteristics; dilatation of superficial and subepithelial vascular network; blue spots corresponding to intramucosal petechiae; micropolyps with a vascular axis
Low-risk hyperplasia	Thick endometrium with no evident or subtle vascular network
High-risk hyperplasia	Thick endometrium or irregular endometrial surface with irregular vessels
Endometrial cancer	Vegetations, profound alterations in mucosal architecture, cerebroid aspects, atypical aspects of vessels

great efforts to establish classifications to help clinicians to better diagnose endometriotic lesions.

The classification of microhysteroscopic images without NBI was raised in 2003, which divided the images into 5 groups: normal hysteroscopy, benign lesion, low-risk hyperplasia, high-risk hyperplasia, and carcinoma (119). On the basis of the above classification, Cicinelli *et al.* proposed a criterion of NBI hysteroscopy, dividing the images into 8 groups: normal proliferative endometrium, polyp, atrophic polyp, myoma, chronic endometritis, low-risk hyperplasia, high-risk hyperplasia, and endometrial cancer (120). The characteristics of each type are listed in *Table* 7.

Using the criteria proposed by Cicinelli *et al.*, Tinelli conducted a multicenter study to validate the accuracy and efficacy of NBI for the diagnosis of endometrial cancer and hyperplasia (121). The result demonstrated that NBI with the criteria listed did in fact improve the recognition of lesions.

The classifications of cervical intraepithelial neoplasia (CIN)

In 2017, Nishiyama *et al.* explored a novel MV classification system to diagnose CIN with NBI using ME (122). The major factors in the study included vascular change, arrangement, and density. This classification categorized the images into 7 types: normal, CIN1, CIN2, CIN3, CIS, minimum invasive cancer (MIC), and invasive cancer (IC).

Meanwhile, 1 year later, Uchita *et al.* found other abnormal characteristics of CIN3 using ME-NBI: light white epithelium (l-WE), heavy white epithelium (h-WE),

and atypical IPCL (123). They found that atypical IPCL can correspond with IPCL classification (14).

Bronchus and lungs

Early in 2003, it was reported that NBI can be used in the differentiating precancerous and cancerous lesions of bronchial mucosa (124). In 2009, Herth *et al.* also reported that NBI can work as a powerful tool to detect early lung cancer (125). They presented a visual classification based on the vascular changes and classified the lesions into 4 grades: normal, abnormal but not suspicious, suspicious of intraepithelial neoplasia, and tumor. In the study, it was found that normal lesions showed normal mucosal vascularity. Suspicious lesions for intraepithelial neoplasia were characterized by ≥3 criteria: capillary loops, dotted vessels, complex vascular networks of tortuous vessels, and abrupt ending vessels. Abnormal but not suspicious lesions showed increased density and <3 criteria mentioned above. Tumors under NBI were visible. This classification has been demonstrated to be useful in the detection of lung cancer (126,127).

Similarly, in 2010, Shibuya *et al.* classified the images into 5 groups: squamous dysplasia, angiogenic squamous dysplasia (ASD), CIS, micro invasive, and invasive. The vessel morphology can be classified into tortuous vessel networks, dotted vessels, and spiral and screw type vessels (128). Squamous dysplasia is characterized by tortuous vessel networks; ASD is characterized by tortuous vessel networks and dotted vessels; CIS, micro invasive, and invasive are observed with dotted vessels, spiral and screw

type vessels. Besides, the mean vessels diameter increased with the progression of lesions.

In 2021, Fukada *et al.* proposed a simple system to classify the bronchoscopic images of peripheral pulmonary tumor (PPT) (129). Based on the appearance of stenosis, the lesions were divided into stenotic type (ST) and non-stenotic type (NonST). According to the presence of epithelium and light blue line (LBL), the lesions were divided into exposed type (ET) and non-exposed type (NonET). They also correlated these types with pathological findings and found that most ST and NonET lesions are commonly shown in adenocarcinoma. Furthermore, ST and ET lesions can be observed in squamous cell carcinoma, whereas all NonST and NonET lesions are found in adenocarcinoma.

Bladder cancer

Studies have reported that NBI can improve the accuracy of the diagnosis of bladder cancer regardless of experience. It has been recommended by the European Association of Urology (EAU) guidelines for non-muscle-invasive urothelial carcinoma (130-136). However, there are few classifications for bladder cancer. In 2018, Dalgaard *et al.* used NBI flexible videoscopy (NBI-FV) to classify the lesions according to the characteristics of microvasculature (geometric pattern, dense, and tortuous and irregular) and mucosa (transparent, thick, and exophytic of papillary). The suspicion was scored from none (score 1) to high (score 5) on the Likert 5-score scale (LS) (137).

Scar

As guidelines recommended, targeted biopsies of resection site are necessary to exclude histopathological evidence of recurrence (138-140). However, with the development of the endoscopic system, it was demonstrated that the mucosal surface could be clearly observed using NBI. Many researchers have tried to set up classifications of scars to avoid unnecessary biopsies.

In 2017, Desomer *et al.* attempted to raise a standardized imaging protocol based on the Kudo's pit pattern and NICE classification used in colorectal lesions (103,105,106,141). Although the results suggested high sensitivity and accuracy, no official classification was raised. Therefore, some researchers developed the narrow-band imaging for scar (NBI-SCAR) classification in 2020 (142). By evacuating the scar with NBI, they described the key characteristics of both recurrent and non-recurrent disease. The features

of recurrence are dark brown color, elongated or branched pit pattern, and dense CP surrounding pits, whereas no recurrence is characterized by a whitish, pale appearance, round, and slightly larger pits compared with the surroundings, and irregular sparse vessels with no change in caliber.

Tips and tricks

As part of optical imaging, NBI uses light characteristics to acquire information on the mucosa and submucosa. Adequate light and a clear field of view are critical to imaging results. Light penetration may be altered by blood and bile, resulting in a black and red image, respectively, which interferes with the evaluation of NBI. To obtain a clear endoscopic view, it is extremely important to avoid bleeding during the examination and to wash the bile (143,144). NBI mainly assesses mucosal surface structures due to its light penetration characteristics. Therefore, all of the above classifications are based on mucosal and submucosal morphological manifestations, especially dynamic changes of IPCLs during tumor progression.

Future prospect and conclusions

With the rapid development of science and technology, artificial intelligence (AI) systems have been increasingly applied for endoscopic diagnosis (145-148). Moreover, studies have demonstrated that AI has a favorable performance with high sensitivity (149-151). Goda *et al.* also predicted that AI may be applied to improve diagnostic criteria for B2 vessels and modify the JES classification (152). At the same time, the combination of the emerging hyperspectral imaging (HSI) technology and AI in recent years has further improved the accuracy of early esophageal cancer detection (153-155). We believe that NBI combined with AI will be widely used in the diagnosis of diseases, and more simple classifications will be used in clinical practice to alleviate the workload of clinicians in the future.

Since the introduction of NBI, many studies have demonstrated its high value in detecting lesions in the early stage of diseases with high accuracy. To date, many studies have focused on NBI classifications in different systems. Most of these classifications share something in common, namely, they all use the characteristics of the vessels as a criterion of classifications. The lesions of different systems also presented unique features under NBI, which may be related to their different pathological changes. Therefore,

more clinical trial validations based on pathology as the gold standard can further promote the accuracy of NBI classification. Moreover, these classifications can also serve as the basis for research on AI diagnostic techniques.

Acknowledgments

Footnote

Reporting Checklist: The authors have completed the Narrative Review reporting checklist. Available at https://qims.amegroups.com/article/view/10.21037/qims-22-728/rc

Conflicts of Interest: All authors have completed the ICMJE uniform disclosure form (available at https://qims.amegroups.com/article/view/10.21037/qims-22-728/coif). The authors have no conflicts of interest to declare.

Ethical Statement: The authors are accountable for all aspects of the work in ensuring that questions related to the accuracy or integrity of any part of the work are appropriately investigated and resolved.

References

1. Soerjomataram I, Bray F. Planning for tomorrow: global cancer incidence and the role of prevention 2020-2070. Nat Rev Clin Oncol 2021;18:663-72.
2. Bray F, Laversanne M, Weiderpass E, Soerjomataram I. The ever-increasing importance of cancer as a leading cause of premature death worldwide. Cancer 2021;127:3029-30.
3. Sung H, Ferlay J, Siegel RL, Laversanne M, Soerjomataram I, Jemal A, Bray F. Global Cancer Statistics 2020: GLOBOCAN Estimates of Incidence and Mortality Worldwide for 36 Cancers in 185 Countries. CA Cancer J Clin 2021;71:209-49.
4. Henley SJ, Ward EM, Scott S, Ma J, Anderson RN, Firth AU, Thomas CC, Islami F, Weir HK, Lewis DR, Sherman RL, Wu M, Benard VB, Richardson LC, Jemal A, Cronin K, Kohler BA. Annual report to the nation on the status of cancer, part I: National cancer statistics. Cancer 2020;126:2225-49.
5. Islami F, Ward EM, Sung H, Cronin KA, Tangka FKL, Sherman RL, Zhao J, Anderson RN, Henley SJ, Yabroff KR, Jemal A, Benard VB. Annual Report to the Nation on the Status of Cancer, Part 1: National Cancer Statistics. J Natl Cancer Inst 2021;113:1648-69.
6. Allemani C, Weir HK, Carreira H, Harewood R, Spika D, Wang XS, et al. Global surveillance of cancer survival 1995-2009: analysis of individual data for 25,676,887 patients from 279 population-based registries in 67 countries (CONCORD-2). Lancet 2015;385:977-1010.
7. Smith RA, Andrews KS, Brooks D, Fedewa SA, Manassaram-Baptiste D, Saslow D, Wender RC. Cancer screening in the United States, 2019: A review of current American Cancer Society guidelines and current issues in cancer screening. CA Cancer J Clin 2019;69:184-210.
8. Ahmed S, Strand S, Weinmann-Menke J, Urbansky L, Galle PR, Neumann H. Molecular endoscopic imaging in cancer. Dig Endosc 2018;30:719-29.
9. Kato T, Iwasaki T, Arihiro S, Saruta M. Endoscopic visualization of cancer and dysplasia in patients with ulcerative colitis following sensitization with oral 5-aminolevulinic acid. J Dig Dis 2020;21:498-504.
10. Nakajima M, Kato H. Image-enhanced endoscopy and magnifying endoscopy for esophageal cancer. Kyobu Geka 2014;67:764-8.
11. Young E, Philpott H, Singh R. Endoscopic diagnosis and treatment of gastric dysplasia and early cancer: Current evidence and what the future may hold. World J Gastroenterol 2021;27:5126-51.
12. Kobayashi S, Yamada M, Takamaru H, Sakamoto T, Matsuda T, Sekine S, Igarashi Y, Saito Y. Diagnostic yield of the Japan NBI Expert Team (JNET) classification for endoscopic diagnosis of superficial colorectal neoplasms in a large-scale clinical practice database. United European Gastroenterol J 2019;7:914-23.
13. Zheng C, Lv Y, Zhong Q, Wang R, Jiang Q. Narrow band imaging diagnosis of bladder cancer: systematic review and meta-analysis. BJU Int 2012;110:E680-7.
14. Inoue H, Kaga M, Ikeda H, Sato C, Sato H, Minami

H, Santi EG, Hayee B, Eleftheriadis N. Magnification endoscopy in esophageal squamous cell carcinoma: a review of the intrapapillary capillary loop classification. Ann Gastroenterol 2015;28:41-8.

15. Takano JH, Yakushiji T, Kamiyama I, Nomura T, Katakura A, Takano N, Shibahara T. Detecting early oral cancer: narrowband imaging system observation of the oral mucosa microvasculature. Int J Oral Maxillofac Surg 2010;39:208-13.

16. Kim DH, Kim Y, Kim SW, Hwang SH. Use of narrowband imaging for the diagnosis and screening of laryngeal cancer: A systematic review and meta-analysis. Head Neck 2020;42:2635-43.

17. Zhou F, Wu L, Huang M, Jin Q, Qin Y, Chen J. The accuracy of magnifying narrow band imaging (ME-NBI) in distinguishing between cancerous and noncancerous gastric lesions: A meta-analysis. Medicine (Baltimore) 2018;97:e9780.

18. Sano Y, Kobayashi M, Hamamoto Y. New diagnostic method based on color imaging using narrow band imaging (NBI) system for gastrointestinal tract. Gastrointestinal Endoscopy 2001;53:AB125.

19. Boscolo Nata F, Tirelli G, Capriotti V, Marcuzzo AV, Sacchet E, Šuran-Brunelli AN, de Manzini N. NBI utility in oncologic surgery: An organ by organ review. Surg Oncol 2021;36:65-75.

20. Gono K, Yamazaki K, Doguchi N, Nonami T, Obi T, Yamaguchi M, Ohyama N, Machida H, Sano Y, Yoshida S, Hamamoto Y, Endo T. Endoscopic Observation of Tissue by Narrowband Illumination. Optical Review 2003;10:211-5.

21. Gono K, Obi T, Yamaguchi M, Ohyama N, Machida H, Sano Y, Yoshida S, Hamamoto Y, Endo T. Appearance of enhanced tissue features in narrow-band endoscopic imaging. J Biomed Opt 2004;9:568-77.

22. Kumagai Y, Inoue H, Nagai K, Kawano T, Iwai T. Magnifying endoscopy, stereoscopic microscopy, and the microvascular architecture of superficial esophageal carcinoma. Endoscopy 2002;34:369-75.

23. Muto M, Minashi K, Yano T, Saito Y, Oda I, Nonaka S, Omori T, Sugiura H, Goda K, Kaise M, Inoue H, Ishikawa H, Ochiai A, Shimoda T, Watanabe H, Tajiri H, Saito D. Early detection of superficial squamous cell carcinoma in the head and neck region and esophagus by narrow band imaging: a multicenter randomized controlled trial. J Clin Oncol 2010;28:1566-72.

24. Kumagai Y, Toi M, Inoue H. Dynamism of tumour vasculature in the early phase of cancer progression:

outcomes from oesophageal cancer research. Lancet Oncol 2002;3:604-10.

25. Funayama A, Maruyama S, Yamazaki M, Al-Eryani K, Shingaki S, Saito C, Cheng J, Saku T. Intraepithelially entrapped blood vessels in oral carcinoma in-situ. Virchows Arch 2012;460:473-80.

26. Watanabe A, Taniguchi M, Tsujie H, Hosokawa M, Fujita M, Sasaki S. The value of narrow band imaging for early detection of laryngeal cancer. Eur Arch Otorhinolaryngol 2009;266:1017-23.

27. Piazza C, Cocco D, De Benedetto L, Del Bon F, Nicolai P, Peretti G. Narrow band imaging and high definition television in the assessment of laryngeal cancer: a prospective study on 279 patients. Eur Arch Otorhinolaryngol 2010;267:409-14.

28. Ni XG, He S, Xu ZG, Gao L, Lu N, Yuan Z, Lai SQ, Zhang YM, Yi JL, Wang XL, Zhang L, Li XY, Wang GQ. Endoscopic diagnosis of laryngeal cancer and precancerous lesions by narrow band imaging. J Laryngol Otol 2011;125:288-96.

29. Ni XG, Zhu JQ, Zhang QQ, Zhang BG, Wang GQ. Diagnosis of vocal cord leukoplakia: The role of a novel narrow band imaging endoscopic classification. Laryngoscope 2019;129:429-34.

30. Arens C, Piazza C, Andrea M, Dikkers FG, Tjon Pian Gi RE, Voigt-Zimmermann S, Peretti G. Proposal for a descriptive guideline of vascular changes in lesions of the vocal folds by the committee on endoscopic laryngeal imaging of the European Laryngological Society. Eur Arch Otorhinolaryngol 2016;273:1207-14.

31. Puxeddu R, Sionis S, Gerosa C, Carta F. Enhanced contact endoscopy for the detection of neoangiogenesis in tumors of the larynx and hypopharynx. Laryngoscope 2015;125:1600-6.

32. Pietruszewska W, Morawska J, Rosiak O, Leduchowska A, Klimza H, Wierzbicka M. Vocal Fold Leukoplakia: Which of the Classifications of White Light and Narrow Band Imaging Most Accurately Predicts Laryngeal Cancer Transformation? Proposition for a Diagnostic Algorithm. Cancers (Basel) 2021;13:3273.

33. Bruno C, Fiori GM, Locatello LG, Cannavicci A, Gallo O, Maggiore G. The role of Narrow Band Imaging (NBI) in the diagnosis of sinonasal diseases. Rhinology 2021;59:40-8.

34. Wen YH, Zhu XL, Lei WB, Zeng YH, Sun YQ, Wen WP. Narrow-band imaging: a novel screening tool for early nasopharyngeal carcinoma. Arch Otolaryngol Head Neck Surg 2012;138:183-8.

35. Lin YC, Watanabe A, Chen WC, Lee KF, Lee IL, Wang WH. Narrowband imaging for early detection of malignant tumors and radiation effect after treatment of head and neck cancer. Arch Otolaryngol Head Neck Surg 2010;136:234-9.

36. Eguchi K, Matsui T, Mukai M, Sugimoto T. Prediction of the depth of invasion in superficial pharyngeal cancer: Microvessel morphological evaluation with narrowband imaging. Head Neck 2019;41:3970-5.

37. Muto M, Nakane M, Katada C, Sano Y, Ohtsu A, Esumi H, Ebihara S, Yoshida S. Squamous cell carcinoma in situ at oropharyngeal and hypopharyngeal mucosal sites. Cancer 2004;101:1375-81.

38. Kikuchi D, Iizuka T, Yamada A, Furuhata T, Yamashita S, Nomura K, Kuribayashi Y, Kimura R, Matsui A, Mitani T, Ogawa O, Takeda H, Hoteya S, Kaise M. Utility of magnifying endoscopy with narrow band imaging in determining the invasion depth of superficial pharyngeal cancer. Head Neck 2015;37:846-50.

39. Goda K, Fujisaki J, Ishihara R, Takeuchi M, Takahashi A, Takaki Y, et al. Newly developed magnifying endoscopic classification of the Japan Esophageal Society to identify superficial Barrett's esophagus-related neoplasms. Esophagus 2018. [Epub ahead of print]. doi: 10.1007/s10388-018-0623-y.

40. Inoue H, Kaga M, Sato Y, Sugaya S, Kudo S. Magnifying Endoscopic Diagnosis of Tissue Atypia and Cancer Invasion Depth in the Area of Pharyngo-Esophageal Squamous Epithelium by NBI Enhanced Magnification Image: IPCL Pattern Classification. In: Cohen J. editor. Comprehensive Atlas of High Resolution Endoscopy and Narrowband Imaging. Malden: MA Blackwell, 2007:49-66.

41. Inoue H. Endoscopic diagnosis of tissue atypism (EA) in the pharyngeal and esophageal squamous epithelium; IPCL pattern classification and ECA classification. Kyobu Geka 2007;60:768-75.

42. Ni XG, Zhang QQ, Wang GQ. Classification of nasopharyngeal microvessels detected by narrow band imaging endoscopy and its role in the diagnosis of nasopharyngeal carcinoma. Acta Otolaryngol 2017;137:546-53.

43. Tirelli G, Marcuzzo AV, Boscolo Nata F. Narrow-band imaging pattern classification in oral cavity. Oral Dis 2018;24:1458-67.

44. Lin YC, Wang WH, Lee KF, Tsai WC, Weng HH. Value of narrow band imaging endoscopy in early mucosal head and neck cancer. Head Neck 2012;34:1574-9.

45. Bansal A, Ulusarac O, Mathur S, Sharma P. Correlation between narrow band imaging and nonneoplastic gastric pathology: a pilot feasibility trial. Gastrointest Endosc 2008;67:210-6.

46. Kaise M, Kato M, Urashima M, Arai Y, Kaneyama H, Kanzazawa Y, Yonezawa J, Yoshida Y, Yoshimura N, Yamasaki T, Goda K, Imazu H, Arakawa H, Mochizuki K, Tajiri H. Magnifying endoscopy combined with narrow-band imaging for differential diagnosis of superficial depressed gastric lesions. Endoscopy 2009;41:310-5.

47. Kadowaki S, Tanaka K, Toyoda H, Kosaka R, Imoto I, Hamada Y, Katsurahara M, Inoue H, Aoki M, Noda T, Yamada T, Takei Y, Katayama N. Ease of early gastric cancer demarcation recognition: a comparison of four magnifying endoscopy methods. J Gastroenterol Hepatol 2009;24:1625-30.

48. Ezoe Y, Muto M, Horimatsu T, Minashi K, Yano T, Sano Y, Chiba T, Ohtsu A. Magnifying narrow-band imaging versus magnifying white-light imaging for the differential diagnosis of gastric small depressive lesions: a prospective study. Gastrointest Endosc 2010;71:477-84.

49. Capelle LG, Haringsma J, de Vries AC, Steyerberg EW, Biermann K, van Dekken H, Kuipers EJ. Narrow band imaging for the detection of gastric intestinal metaplasia and dysplasia during surveillance endoscopy. Dig Dis Sci 2010;55:3442-8.

50. Okubo M, Tahara T, Shibata T, Nakamura M, Yoshioka D, Maeda Y, Yonemura J, Ishizuka T, Arisawa T, Hirata I. Changes in gastric mucosal patterns seen by magnifying NBI during H. pylori eradication. J Gastroenterol 2011;46:175-82.

51. Kikuchi D, Iizuka T, Hoteya S, Yamada A, Furuhata T, Yamashita S, Domon K, Nakamura M, Matsui A, Mitani T, Ogawa O, Watanabe S, Kaise M. Usefulness of magnifying endoscopy with narrow-band imaging for determining tumor invasion depth in early gastric cancer. Gastroenterol Res Pract 2013;2013:217695.

52. Yoshida T, Inoue H, Usui S, Satodate H, Fukami N, Kudo SE. Narrow-band imaging system with magnifying endoscopy for superficial esophageal lesions. Gastrointest Endosc 2004;59:288-95.

53. Inoue H, Honda T, Nagai K, Kawano T, Yoshino K, Takeshita K, Endo M. Ultra high Magnification Endoscopic Observation of Carcinoma in situ of the Esophagus. Digestive Endoscopy 1997;9. doi: 10.1111/j.1443-1661.1997.tb00453.x.

54. Inoue H. Magnification endoscopy in the esophagus and stomach. Digestive Endoscopy 2001;13:S40-1.

55. Arima M, Tada M, Arima H. Evaluation of microvascular

patterns of superficial esophageal cancers by magnifying endoscopy. Esophagus 2005;2:191-7.

56. Oyama T, Inoue H, Arima M, Momma K, Omori T, Ishihara R, Hirasawa D, Takeuchi M, Tomori A, Goda K. Prediction of the invasion depth of superficial squamous cell carcinoma based on microvessel morphology: magnifying endoscopic classification of the Japan Esophageal Society. Esophagus 2017;14:105-12.

57. Qumseya BJ, Wang H, Badie N, Uzomba RN, Parasa S, White DL, Wolfsen H, Sharma P, Wallace MB. Advanced imaging technologies increase detection of dysplasia and neoplasia in patients with Barrett's esophagus: a meta-analysis and systematic review. Clin Gastroenterol Hepatol 2013;11:1562-70.e1-2.

58. Kara MA, Ennahachi M, Fockens P, ten Kate FJ, Bergman JJ. Detection and classification of the mucosal and vascular patterns (mucosal morphology) in Barrett's esophagus by using narrow band imaging. Gastrointest Endosc 2006;64:155-66.

59. Sharma P, Bansal A, Mathur S, Wani S, Cherian R, McGregor D, Higbee A, Hall S, Weston A. The utility of a novel narrow band imaging endoscopy system in patients with Barrett's esophagus. Gastrointest Endosc 2006;64:167-75.

60. Singh R, Anagnostopoulos GK, Yao K, Karageorgiou H, Fortun PJ, Shonde A, Garsed K, Kaye PV, Hawkey CJ, Ragunath K. Narrow-band imaging with magnification in Barrett's esophagus: validation of a simplified grading system of mucosal morphology patterns against histology. Endoscopy 2008;40:457-63.

61. Sharma P, Mathur S, Dixon A, Weston A. arrow Band Imaging Endoscopy for the Detection of Dysplastic and Non Dysplastic Barrett's Esophagus. Gastrointestinal Endoscopy 2004;59:P263.

62. Mannath J, Subramanian V, Hawkey CJ, Ragunath K. Narrow band imaging for characterization of high grade dysplasia and specialized intestinal metaplasia in Barrett's esophagus: a meta-analysis. Endoscopy 2010;42:351-9.

63. Goda K, Tajiri H, Ikegami M, Urashima M, Nakayoshi T, Kaise M. Usefulness of magnifying endoscopy with narrow band imaging for the detection of specialized intestinal metaplasia in columnar-lined esophagus and Barrett's adenocarcinoma. Gastrointest Endosc 2007;65:36-46.

64. Silva FB, Dinis-Ribeiro M, Vieth M, Rabenstein T, Goda K, Kiesslich R, Haringsma J, Edebo A, Toth E, Soares J, Areia M, Lundell L, Marschall HU. Endoscopic assessment and grading of Barrett's esophagus using magnification endoscopy and narrow-band imaging:

accuracy and interobserver agreement of different classification systems (with videos). Gastrointest Endosc 2011;73:7-14.

65. Uno G, Ishimura N, Tada Y, Tamagawa Y, Yuki T, Matsushita T, Ishihara S, Amano Y, Maruyama R, Kinoshita Y. Simplified classification of capillary pattern in Barrett esophagus using magnifying endoscopy with narrow band imaging: implications for malignant potential and interobserver agreement. Medicine (Baltimore) 2015;94:e405.

66. Anagnostopoulos GK, Yao K, Kaye P, Hawkey CJ, Ragunath K. Novel endoscopic observation in Barrett's oesophagus using high resolution magnification endoscopy and narrow band imaging. Aliment Pharmacol Ther 2007;26:501-7.

67. Sharma P, Bergman JJ, Goda K, Kato M, Messmann H, Alsop BR, Gupta N, Vennalaganti P, Hall M, Konda V, Koons A, Penner O, Goldblum JR, Waxman I. Development and Validation of a Classification System to Identify High-Grade Dysplasia and Esophageal Adenocarcinoma in Barrett's Esophagus Using Narrow-Band Imaging. Gastroenterology 2016;150:591-8.

68. Yao K, Oishi T, Matsui T, Yao T, Iwashita A. Novel magnified endoscopic findings of microvascular architecture in intramucosal gastric cancer. Gastrointest Endosc 2002;56:279-84.

69. Yao K, Oishi T. Microgastroscopic findings of mucosal microvascular architecture as visualized by magnifying endoscopy. Dig Endosc 2001;13:S27-33.

70. Yao K, Yao T, Iwashita A. Determining the horizontal extent of early gastric carcinoma: two modern techniques based on differences in the mucosal microvascular architecture and density between carcinomatous and non-carcinomatous mucosa. Dig Endosc 2002;14:S83-7.

71. Yao K, Anagnostopoulos GK, Ragunath K. Magnifying endoscopy for diagnosing and delineating early gastric cancer. Endoscopy 2009;41:462-7.

72. Nakayoshi T, Tajiri H, Matsuda K, Kaise M, Ikegami M, Sasaki H. Magnifying endoscopy combined with narrow band imaging system for early gastric cancer: correlation of vascular pattern with histopathology (including video). Endoscopy 2004;36:1080-4.

73. Yokoyama A, Inoue H, Minami H, Wada Y, Sato Y, Satodate H, Hamatani S, Kudo SE. Novel narrow-band imaging magnifying endoscopic classification for early gastric cancer. Dig Liver Dis 2010;42:704-8.

74. Inoue H, Kodama K, Minami H, Wada Y, Kaga M, Sato Y, Sugaya S, Kudo S. NBI magnifying endoscopic

classification using crystal violet staining. Nihon Rinsho 2008;66:1023-7.

75. Ribeiro H, Libânio D, Castro R, Ferreira A, Barreiro P, Boal Carvalho P, Capela T, Pimentel-Nunes P, Santos C, Dinis-Ribeiro M. Reliability of Paris Classification for superficial neoplastic gastric lesions improves with training and narrow band imaging. Endosc Int Open 2019;7:E633-40.

76. Update on the paris classification of superficial neoplastic lesions in the digestive tract. Endoscopy 2005;37:570-8.

77. Tamai N, Kaise M, Nakayoshi T, Katoh M, Sumiyama K, Gohda K, Yamasaki T, Arakawa H, Tajiri H. Clinical and endoscopic characterization of depressed gastric adenoma. Endoscopy 2006;38:391-4.

78. Yao K, Iwashita A, Tanabe H, Nishimata N, Nagahama T, Maki S, Takaki Y, Hirai F, Hisabe T, Nishimura T, Matsui T. White opaque substance within superficial elevated gastric neoplasia as visualized by magnification endoscopy with narrow-band imaging: a new optical sign for differentiating between adenoma and carcinoma. Gastrointest Endosc 2008;68:574-80.

79. Schlemper RJ, Riddell RH, Kato Y, Borchard F, Cooper HS, Dawsey SM, et al. The Vienna classification of gastrointestinal epithelial neoplasia. Gut 2000;47:251-5.

80. The Paris endoscopic classification of superficial neoplastic lesions: esophagus, stomach, and colon: November 30 to December 1, 2002. Gastrointest Endosc 2003;58:S3-43.

81. Nakamura M, Shibata T, Tahara T, Yoshioka D, Okubo M, Mizoguchi Y, Kuroda M, Arisawa T, Hirata I. The usefulness of magnifying endoscopy with narrow-band imaging to distinguish carcinoma in flat elevated lesions in the stomach diagnosed as adenoma by using biopsy samples. Gastrointest Endosc 2010;71:1070-5.

82. Kobayashi M, Hashimoto S, Nishikura K, Mizuno K, Takeuchi M, Ajioka Y. Assessment of gastric phenotypes using magnifying narrow-band imaging for differentiation of gastric carcinomas from adenomas. Gastroenterol Res Pract 2014;2014:274301.

83. Pimentel-Nunes P, Dinis-Ribeiro M, Soares JB, Marcos-Pinto R, Santos C, Rolanda C, Bastos RP, Areia M, Afonso L, Bergman J, Sharma P, Gotoda T, Henrique R, Moreira-Dias L. A multicenter validation of an endoscopic classification with narrow band imaging for gastric precancerous and cancerous lesions. Endoscopy 2012;44:236-46.

84. Uchiyama Y, Imazu H, Kakutani H, Hino S, Sumiyama K, Kuramochi A, Tsukinaga S, Matsunaga K, Nakayoshi T, Goda K, Saito S, Kaise M, Kawamuara M, Omar S,

Tajiri H. New approach to diagnosing ampullary tumors by magnifying endoscopy combined with a narrow-band imaging system. J Gastroenterol 2006;41:483-90.

85. Park JS, Seo DW, Song TJ, Park DH, Lee SS, Lee SK, Kim MH. Usefulness of white-light imaging-guided narrow-band imaging for the differential diagnosis of small ampullary lesions. Gastrointest Endosc 2015;82:94-101.

86. Akazawa Y, Ueyama H, Tsuyama S, Ikeda A, Yatagai N, Komori H, Takeda T, Matsumoto K, Matsumoto K, Hashimoto T, Tomita N, Kajiyama Y, Kato M, Yao T, Nagahara A. Endoscopic and Clinicopathological Features of Superficial Non-Ampullary Duodenal Tumor Based on the Mucin Phenotypes. Digestion 2021;102:663-70.

87. Tanaka Y, Fujii S, Oiwa Y, Kusaka T, Shibuya S, Kokuryu H. Efficacy of Magnifying Narrow Band Imaging with Acetic Acid Spray in Diagnosing Superficial Non-Ampullary Duodenal Epithelial Tumors. Digestion 2021;102:572-9.

88. Yoshimura N, Goda K, Tajiri H, Ikegami M, Nakayoshi T, Kaise M. Endoscopic features of nonampullary duodenal tumors with narrow-band imaging. Hepatogastroenterology 2010;57:462-7.

89. Kikuchi D, Hoteya S, Iizuka T, Kimura R, Kaise M. Diagnostic algorithm of magnifying endoscopy with narrow band imaging for superficial non-ampullary duodenal epithelial tumors. Dig Endosc 2014;26 Suppl 2:16-22.

90. Dixon MF. Gastrointestinal epithelial neoplasia: Vienna revisited. Gut 2002;51:130-1.

91. Tsuji S, Doyama H, Tsuji K, Tsuyama S, Tominaga K, Yoshida N, Takemura K, Yamada S, Niwa H, Katayanagi K, Kurumaya H, Okada T. Preoperative endoscopic diagnosis of superficial non-ampullary duodenal epithelial tumors, including magnifying endoscopy. World J Gastroenterol 2015;21:11832-41.

92. Stolte M. The new Vienna classification of epithelial neoplasia of the gastrointestinal tract: advantages and disadvantages. Virchows Arch 2003;442:99-106.

93. Mizumoto T, Sanomura Y, Tanaka S, Kuroki K, Kurihara M, Yoshifuku Y, Oka S, Arihiro K, Shimamoto F, Chayama K. Clinical usefulness of magnifying endoscopy for non-ampullary duodenal tumors. Endosc Int Open 2017;5:E297-302.

94. Kakushima N, Yoshida M, Yamaguchi Y, Takizawa K, Kawata N, Tanaka M, Kishida Y, Ito S, Imai K, Hotta K, Ishiwatari H, Matsubayashi H, Sasaki K, Ono H. Magnified endoscopy with narrow-band imaging for the differential diagnosis of superficial non-ampullary

duodenal epithelial tumors. Scand J Gastroenterol 2019;54:128-34.

95. Uraoka T, Saito Y, Matsuda T, Sano Y, Ikehara H, Mashimo Y, Kikuchi T, Saito D, Saito H. Detectability of colorectal neoplastic lesions using a narrow-band imaging system: a pilot study. J Gastroenterol Hepatol 2008;23:1810-5.

96. Inoue T, Murano M, Murano N, Kuramoto T, Kawakami K, Abe Y, Morita E, Toshina K, Hoshiro H, Egashira Y, Umegaki E, Higuchi K. Comparative study of conventional colonoscopy and pan-colonic narrow-band imaging system in the detection of neoplastic colonic polyps: a randomized, controlled trial. J Gastroenterol 2008;43:45-50.

97. Sikka S, Ringold DA, Jonnalagadda S, Banerjee B. Comparison of white light and narrow band high definition images in predicting colon polyp histology, using standard colonoscopes without optical magnification. Endoscopy 2008;40:818-22.

98. Tanaka S, Sano Y. Aim to unify the narrow band imaging (NBI) magnifying classification for colorectal tumors: current status in Japan from a summary of the consensus symposium in the 79th Annual Meeting of the Japan Gastroenterological Endoscopy Society. Dig Endosc 2011;23 Suppl 1:131-9.

99. Ikematsu H, Matsuda T, Emura F, Saito Y, Uraoka T, Fu KI, Kaneko K, Ochiai A, Fujimori T, Sano Y. Efficacy of capillary pattern type IIIA/IIIB by magnifying narrow band imaging for estimating depth of invasion of early colorectal neoplasms. BMC Gastroenterol 2010;10:33.

100. Oba S, Tanaka S, Oka S, Kanao H, Yoshida S, Shimamoto F, Chayama K. Characterization of colorectal tumors using narrow-band imaging magnification: combined diagnosis with both pit pattern and microvessel features. Scand J Gastroenterol 2010;45:1084-92.

101. Kanao H, Tanaka S, Oka S, Hirata M, Yoshida S, Chayama K. Narrow-band imaging magnification predicts the histology and invasion depth of colorectal tumors. Gastrointest Endosc 2009;69:631-6.

102. Wada Y, Kudo SE, Kashida H, Ikehara N, Inoue H, Yamamura F, Ohtsuka K, Hamatani S. Diagnosis of colorectal lesions with the magnifying narrow-band imaging system. Gastrointest Endosc 2009;70:522-31.

103. Hewett DG, Kaltenbach T, Sano Y, Tanaka S, Saunders BP, Ponchon T, Soetikno R, Rex DK. Validation of a simple classification system for endoscopic diagnosis of small colorectal polyps using narrow-band imaging. Gastroenterology 2012;143:599-607.e1.

104. Hayashi N, Tanaka S, Hewett DG, Kaltenbach TR, Sano Y, Ponchon T, Saunders BP, Rex DK, Soetikno RM. Endoscopic prediction of deep submucosal invasive carcinoma: validation of the narrow-band imaging international colorectal endoscopic (NICE) classification. Gastrointest Endosc 2013;78:625-32.

105. Kudo S, Tamura S, Nakajima T, Yamano H, Kusaka H, Watanabe H. Diagnosis of colorectal tumorous lesions by magnifying endoscopy. Gastrointest Endosc 1996;44:8-14.

106. Kudo S, Hirota S, Nakajima T, Hosobe S, Kusaka H, Kobayashi T, Himori M, Yagyuu A. Colorectal tumours and pit pattern. J Clin Pathol 1994;47:880-5.

107. Hirata M, Tanaka S, Oka S, Kaneko I, Yoshida S, Yoshihara M, Chayama K. Magnifying endoscopy with narrow band imaging for diagnosis of colorectal tumors. Gastrointest Endosc 2007;65:988-95.

108. Hayashi N, Tanaka S, Kanao H, Oka S, Yoshida S, Chayama K. Relationship between narrow-band imaging magnifying observation and pit pattern diagnosis in colorectal tumors. Digestion 2013;87:53-8.

109. Sano Y, Tanaka S, Kudo SE, Saito S, Matsuda T, Wada Y, et al. Narrow-band imaging (NBI) magnifying endoscopic classification of colorectal tumors proposed by the Japan NBI Expert Team. Dig Endosc 2016;28:526-33.

110. Iwatate M, Sano Y, Tanaka S, Kudo SE, Saito S, Matsuda T, et al. Validation study for development of the Japan NBI Expert Team classification of colorectal lesions. Dig Endosc 2018;30:642-51.

111. IJspeert JE, Bastiaansen BA, van Leerdam ME, Meijer GA, van Eeden S, Sanduleanu S, Schoon EJ, Bisseling TM, Spaander MC, van Lelyveld N, Bargeman M, Wang J, Dekker E; . Development and validation of the WASP classification system for optical diagnosis of adenomas, hyperplastic polyps and sessile serrated adenomas/polyps. Gut 2016;65:963-70.

112. Hazewinkel Y, López-Cerón M, East JE, Rastogi A, Pellisé M, Nakajima T, van Eeden S, Tytgat KM, Fockens P, Dekker E. Endoscopic features of sessile serrated adenomas: validation by international experts using high-resolution white-light endoscopy and narrow-band imaging. Gastrointest Endosc 2013;77:916-24.

113. Sumimoto K, Tanaka S, Shigita K, Hayashi N, Hirano D, Tamaru Y, Ninomiya Y, Oka S, Arihiro K, Shimamoto F, Yoshihara M, Chayama K. Diagnostic performance of Japan NBI Expert Team classification for differentiation among noninvasive, superficially invasive, and deeply invasive colorectal neoplasia. Gastrointest Endosc 2017;86:700-9.

114. Yamaguchi T, Hara T, Tsuyuguchi T, Ishihara T, Tsuchiya S, Saitou M, Saisho H. Peroral pancreatoscopy in the diagnosis of mucin-producing tumors of the pancreas. Gastrointest Endosc 2000;52:67-73.

115. Miura T, Igarashi Y, Okano N, Miki K, Okubo Y. Endoscopic diagnosis of intraductal papillary-mucinous neoplasm of the pancreas by means of peroral pancreatoscopy using a small-diameter videoscope and narrow-band imaging. Dig Endosc 2010;22:119-23.

116. Mounzer R, Austin GL, Wani S, Brauer BC, Fukami N, Shah RJ. Per-oral video cholangiopancreatoscopy with narrow-band imaging for the evaluation of indeterminate pancreaticobiliary disease. Gastrointest Endosc 2017;85:509-17.

117. Farrugia M, Nair MS, Kotronis KV. Narrow band imaging in endometriosis. J Minim Invasive Gynecol 2007;14:393-4.

118. Surico D, Vigone A, Leo L. Narrow band imaging in endometrial lesions. J Minim Invasive Gynecol 2009;16:9-10.

119. Dotto JE, Lema B, Dotto JE Jr, Hamou J. Classification of microhysteroscopic images and their correlation with histologic diagnoses. J Am Assoc Gynecol Laparosc 2003;10:233-46.

120. Cicinelli E, Tinelli R, Colafiglio G, Pastore A, Mastrolia S, Lepera A, Clevin L. Reliability of narrow-band imaging (NBI) hysteroscopy: a comparative study. Fertil Steril 2010;94:2303-7.

121. Tinelli R, Surico D, Leo L, Pinto V, Surico N, Fusco A, Cicinelli MV, Meir YJ, Cicinelli E. Accuracy and efficacy of narrow-band imaging versus white light hysteroscopy for the diagnosis of endometrial cancer and hyperplasia: a multicenter controlled study. Menopause 2011;18:1026-9.

122. Nishiyama N, Kanenishi K, Mori H, Kobara H, Fujihara S, Chiyo T, Kobayashi N, Matsunaga T, Ayaki M, Yachida T, Fujimori A, Oryu M, Tenkumo C, Ishibashi M, Hanaoka U, Hata T, Miyai Y, Kadota K, Haba R, Masaki T. Flexible magnifying endoscopy with narrow band imaging for the diagnosis of uterine cervical tumors: A cooperative study among gastrointestinal endoscopists and gynecologists to explore a novel microvascular classification system. Oncol Lett 2017;14:355-62.

123. Uchita K, Kanenishi K, Hirano K, Kobara H, Nishiyama N, Kawada A, Fujihara S, Ibuki E, Haba R, Takahashi Y, Kai Y, Yorita K, Mori H, Kunikata J, Nishimoto N, Hata T, Masaki T. Characteristic findings of high-grade cervical intraepithelial neoplasia or more on magnifying endoscopy with narrow band imaging. Int J Clin Oncol 2018;23:707-14.

124. Shibuya K, Hoshino H, Chiyo M, Iyoda A, Yoshida S, Sekine Y, Iizasa T, Saitoh Y, Baba M, Hiroshima K, Ohwada H, Fujisawa T. High magnification bronchovideoscopy combined with narrow band imaging could detect capillary loops of angiogenic squamous dysplasia in heavy smokers at high risk for lung cancer. Thorax 2003;58:989-95.

125. Herth FJ, Eberhardt R, Anantham D, Gompelmann D, Zakaria MW, Ernst A. Narrow-band imaging bronchoscopy increases the specificity of bronchoscopic early lung cancer detection. J Thorac Oncol 2009;4:1060-5.

126. Zaric B, Perin B, Stojsic V, Carapic V, Eri Z, Panjkovic M, Andrijevic I, Matijasevic J. Relation between vascular patterns visualized by Narrow Band Imaging (NBI) videobronchoscopy and histological type of lung cancer. Med Oncol 2013;30:374.

127. Vincent BD, Fraig M, Silvestri GA. A pilot study of narrow-band imaging compared to white light bronchoscopy for evaluation of normal airways and premalignant and malignant airways disease. Chest 2007;131:1794-9.

128. Shibuya K, Nakajima T, Fujiwara T, Chiyo M, Hoshino H, Moriya Y, Suzuki M, Hiroshima K, Nakatani Y, Yoshino I. Narrow band imaging with high-resolution bronchovideoscopy: a new approach for visualizing angiogenesis in squamous cell carcinoma of the lung. Lung Cancer 2010;69:194-202.

129. Fukada T, Morita K, Kurimoto N, Setoguchi M, Nosaka S, Katsumata T. The Usefulness of a Simple Classification for Bronchoscopic Findings for Diagnosis of Peripheral Pulmonary Tumour. Respiration 2021;100:794-803.

130. Bryan RT, Billingham LJ, Wallace DM. Narrow-band imaging flexible cystoscopy in the detection of recurrent urothelial cancer of the bladder. BJU Int 2008;101:702-5; discussion 705-6.

131. Bryan RT, Shah ZH, Collins SI, Wallace DM. Narrow-band imaging flexible cystoscopy: a new user's experience. J Endourol 2010;24:1339-43.

132. Herr HW, Donat SM. A comparison of white-light cystoscopy and narrow-band imaging cystoscopy to detect bladder tumour recurrences. BJU Int 2008;102:1111-4.

133. Naselli A, Introini C, Bertolotto F, Spina B, Puppo P. Narrow band imaging for detecting residual/recurrent cancerous tissue during second transurethral resection of newly diagnosed non-muscle-invasive high-grade bladder cancer. BJU Int 2010;105:208-11.

134. Babjuk M, Böhle A, Burger M, Capoun O, Cohen D,

Compérat EM, Hernández V, Kaasinen E, Palou J, Rouprêt M, van Rhijn BWG, Shariat SF, Soukup V, Sylvester RJ, Zigeuner R. EAU Guidelines on Non-Muscle-invasive Urothelial Carcinoma of the Bladder: Update 2016. Eur Urol 2017;71:447-61.

135. Cauberg EC, Kloen S, Visser M, de la Rosette JJ, Babjuk M, Soukup V, Pesl M, Duskova J, de Reijke TM. Narrow band imaging cystoscopy improves the detection of non-muscle-invasive bladder cancer. Urology 2010;76:658-63.

136. Chen G, Wang B, Li H, Ma X, Shi T, Zhang X. Applying narrow-band imaging in complement with white-light imaging cystoscopy in the detection of urothelial carcinoma of the bladder. Urol Oncol 2013;31:475-9.

137. Dalgaard LP, Zare R, Gaya JM, Redorta JP, Roumiguié M, Filleron T, Malavaud B. Prospective evaluation of the performances of narrow-band imaging flexible videoscopy relative to white-light imaging flexible videoscopy, in patients scheduled for transurethral resection of a primary NMIBC. World J Urol 2019;37:1615-21.

138. Ferlitsch M, Moss A, Hassan C, Bhandari P, Dumonceau JM, Paspatis G, et al. Colorectal polypectomy and endoscopic mucosal resection (EMR): European Society of Gastrointestinal Endoscopy (ESGE) Clinical Guideline. Endoscopy 2017;49:270-97.

139. Hwang JH, Konda V, Abu Dayyeh BK, Chauhan SS, Enestvedt BK, Fujii-Lau LL, Komanduri S, Maple JT, Murad FM, Pannala R, Thosani NC, Banerjee S. Endoscopic mucosal resection. Gastrointest Endosc 2015;82:215-26.

140. Knabe M, Pohl J, Gerges C, Ell C, Neuhaus H, Schumacher B. Standardized long-term follow-up after endoscopic resection of large, nonpedunculated colorectal lesions: a prospective two-center study. Am J Gastroenterol 2014;109:183-9.

141. Desomer L, Tutticci N, Tate DJ, Williams SJ, McLeod D, Bourke MJ. A standardized imaging protocol is accurate in detecting recurrence after EMR. Gastrointest Endosc 2017;85:518-26.

142. Zorron Cheng Tao Pu L, Chiam KH, Yamamura T, Nakamura M, Berzin TM, Mir FF, Hourneaux de Moura EG, Madruga Neto AC, Koay DSC, Loong CK, Ovenden A, Edwards S, Burt AD, Hirooka Y, Fujishiro M, Singh R. Narrow-band imaging for scar (NBI-SCAR) classification: from conception to multicenter validation. Gastrointest Endosc 2020;91:1146-1154.e5.

143. Mukherjee P, George AJP, Yadav BK, Jeyaseelan L, Kumar RM, Mukha RP, Chandrasingh J, Kumar S, Kekre NS, Devasia A. The Impact of Narrow Band Imaging in the Detection and Resection of Bladder Tumor in Transitional Cell Carcinoma of the Bladder: A Prospective, Blinded, Sequential Intervention Randomized Controlled Trial. Urology 2019;128:55-61.

144. Choi HJ, Moon JH, Lee YN. Advanced Imaging Technology in Biliary Tract Diseases:Narrow-Band Imaging of the Bile Duct. Clin Endosc 2015;48:498-502.

145. Gulati S, Patel M, Emmanuel A, Haji A, Hayee B, Neumann H. The future of endoscopy: Advances in endoscopic image innovations. Dig Endosc 2020;32:512-22.

146. Mori Y, Kudo SE, Mohmed HEN, Misawa M, Ogata N, Itoh H, Oda M, Mori K. Artificial intelligence and upper gastrointestinal endoscopy: Current status and future perspective. Dig Endosc 2019;31:378-88.

147. Olveres J, González G, Torres F, Moreno-Tagle JC, Carbajal-Degante E, Valencia-Rodríguez A, Méndez-Sánchez N, Escalante-Ramírez B. What is new in computer vision and artificial intelligence in medical image analysis applications. Quant Imaging Med Surg 2021;11:3830-53.

148. Ng D, Du H, Yao MM, Kosik RO, Chan WP, Feng M. Today's radiologists meet tomorrow's AI: the promises, pitfalls, and unbridled potential. Quant Imaging Med Surg 2021;11:2775-9.

149. Ohmori M, Ishihara R, Aoyama K, Nakagawa K, Iwagami H, Matsuura N, Shichijo S, Yamamoto K, Nagaike K, Nakahara M, Inoue T, Aoi K, Okada H, Tada T. Endoscopic detection and differentiation of esophageal lesions using a deep neural network. Gastrointest Endosc 2020;91:301-309.e1.

150. Guo L, Xiao X, Wu C, Zeng X, Zhang Y, Du J, Bai S, Xie J, Zhang Z, Li Y, Wang X, Cheung O, Sharma M, Liu J, Hu B. Real-time automated diagnosis of precancerous lesions and early esophageal squamous cell carcinoma using a deep learning model (with videos). Gastrointest Endosc 2020;91:41-51.

151. Nakagawa K, Ishihara R, Aoyama K, Ohmori M, Nakahira H, Matsuura N, Shichijo S, Nishida T, Yamada T, Yamaguchi S, Ogiyama H, Egawa S, Kishida O, Tada T. Classification for invasion depth of esophageal squamous cell carcinoma using a deep neural network compared with experienced endoscopists. Gastrointest Endosc 2019;90:407-14.

152. Goda K, Irisawa A. Japan Esophageal Society classification for predicting the invasion depth of superficial esophageal squamous cell carcinoma: Should it be modified now? Dig Endosc 2020;32:37-8.

153. Tsai CL, Mukundan A, Chung CS, Chen YH, Wang

YK, Chen TH, Tseng YS, Huang CW, Wu IC, Wang HC. Hyperspectral Imaging Combined with Artificial Intelligence in the Early Detection of Esophageal Cancer. Cancers (Basel) 2021;13:4593.

154. Fang YJ, Mukundan A, Tsao YM, Huang CW, Wang HC. Identification of Early Esophageal Cancer by Semantic Segmentation. J Pers Med 2022;12:1204.

155. Wang YK, Syu HY, Chen YH, Chung CS, Tseng YS, Ho SY, Huang CW, Wu IC, Wang HC. Endoscopic Images by a Single-Shot Multibox Detector for the Identification of Early Cancerous Lesions in the Esophagus: A Pilot Study. Cancers (Basel) 2021;13:321.